

Deposition of cenomanian – Turonian organic-rich units on the mid-Norwegian margin: Controlling factors and regional implications

A. Hagset^{a,*}, S.-A. Grundvåg^{a,b}, B. Badics^c, R. Davies^c, A. Rotevatn^d

^a Department of Geosciences, UiT - the Arctic University of Norway, Tromsø, Norway

^b Department of Arctic Geology, University Centre in Svalbard, PO Box 156, 9171, Longyearbyen, Norway

^c Wintershall DEA, Stavanger, Norway

^d Department of Geosciences, University of Bergen, Bergen, Norway

ARTICLE INFO

Keywords:

Lower cretaceous stratigraphy
Mid-Norwegian margin
Cenomanian/Turonian boundary
Seismic sequences
Organic-rich units
Source rock evaluation
Rift-basin configuration
OAE 2
Sedimentation rate

ABSTRACT

On the mid-Norwegian margin, extensive rifting and subsequent deposition of thick Cretaceous and Cenozoic sediments have buried the traditional Upper Jurassic organic-rich shales too deep. Consequently, these organic-rich shales are overmature and spent in the deep basins on the mid-Norwegian margin. The absence of well-control, variable seismic quality and in particular, the great burial depth, makes it difficult to identify alternative Upper Jurassic and Lower Cretaceous organic-rich units. By combining high-resolution 2D seismic data, well logs, and Rock-Eval data, this study documents the presence of alternative organic-rich units in the Cretaceous succession on the Halten Terrace and the Vøring Basin. Multiple seismic horizons which correspond to regional flooding surfaces and define a series of seismic sequences have been mapped across the study area. The regionally extensive upper Cenomanian horizon is associated with wireline log signals and Rock-Eval parameters which imply the presence of a potential source rock unit. Source rock evaluation indicate that this unit contains mainly kerogen Type III on the Halten Terrace, suggesting an organofacies with significant contribution from terrestrial sources. In the Vøring Basin, the unit is sparsely drilled but appears to be mature, thus displaying a relatively limited potential. One well from the Vigrid Syncline demonstrate somewhat higher potential, with Rock-Eval data indicating a kerogen Type II composition. As such, more prolific units seems to exist in the Vøring Basin, albeit exhibiting a patchy distribution. We speculate that the deposition and preservation of this upper Cenomanian organic-rich unit record the development of an extended oxygen minimum zone attributable to increased primary production and sluggish water circulation, linked to the global Oceanic Anoxic Event 2 (OAE 2). However, local physiographic conditions, such as high sedimentation rates, erosion by gravity flows and periodically oxygenated conditions hindered preservation of a significant quantities of organic matter, thus limiting the thickness and quality of the upper Cenomanian organic-rich unit on the mid-Norwegian margin.

1. Introduction

Identifying and mapping the distribution of thermally mature source rock units is important to eliminate risk in hydrocarbon exploration. Whether a viable source rock developed or not, is the outcome of the interaction of many factors and processes across multiple time scales, ultimately recording the environmental and sedimentary response to tectonic, eustatic and climatic forcing (e.g. Arthur and Sageman, 1994; Demaison and Moore, 1980; Demaison et al., 1983; Katz, 2005; Bohacs et al., 2005). The generation and preservation of organic matter, are among other factors, controlled by primary organic production, sedimentation rate, as well as water mass circulation and bottom water

oxygen levels, whereas source rock thermal maturity and thus source rock generation potential, is largely governed by the thermal and burial history of the basin (Demaison et al., 1983; Pedersen and Calvert, 1990; Arthur and Sageman, 1994; Peters and Cassa, 1994; Calvert et al., 1996; Katz, 2005). Therefore, the tectono-sedimentary evolution of a basin needs to be carefully assessed during any source rock evaluation program.

In the Vøring Basin, of the mid-Norwegian margin, the traditional Upper Jurassic source rock (i.e. the Spekk Formation) is classified as over-mature due to deep burial caused by extensive rifting and crustal thinning in the Late Jurassic – Early Cretaceous, and subsequent deposition of several kilometers thick Cretaceous and Cenozoic sediments (e.

* Corresponding author.

E-mail address: aha155@uit.no (A. Hagset).

<https://doi.org/10.1016/j.marpetgeo.2023.106102>

Received 17 November 2022; Received in revised form 4 January 2023; Accepted 7 January 2023

Available online 10 January 2023

0264-8172/© 2023 The Authors. Published by Elsevier Ltd. This is an open access article under the CC BY license (<http://creativecommons.org/licenses/by/4.0/>).

g. Doré et al., 1999; Brekke, 2000; Zastrozhnov et al., 2020). In addition, limited well-control and variable seismic quality due to complex fault geometries and, particularly, great burial depths (i.e. 6 – 9 s TWT; Brekke, 2000; Zastrozhnov et al., 2020) make it difficult to identify alternative Upper Jurassic and Lower Cretaceous organic-rich units in the deepest parts of the basin. As a result, exploration strategies in the area have focused on plays with younger source rocks, particularly those

of Late Cretaceous and Palaeocene age (e.g. Doré et al., 1997b; Brekke et al., 1999; Mann et al., 2002). Although a thermally mature source rock unit has yet to be proven in the Cretaceous succession in the Vøring Basin, biomarker components found in hydrocarbons from the Ellida, Ormen Lange and Snefrid Nord discoveries strongly suggest the presence of a post-Jurassic source rock (Garner et al., 2017; Matapour and Karlsen, 2018). One such potential source rock unit may be organic rich

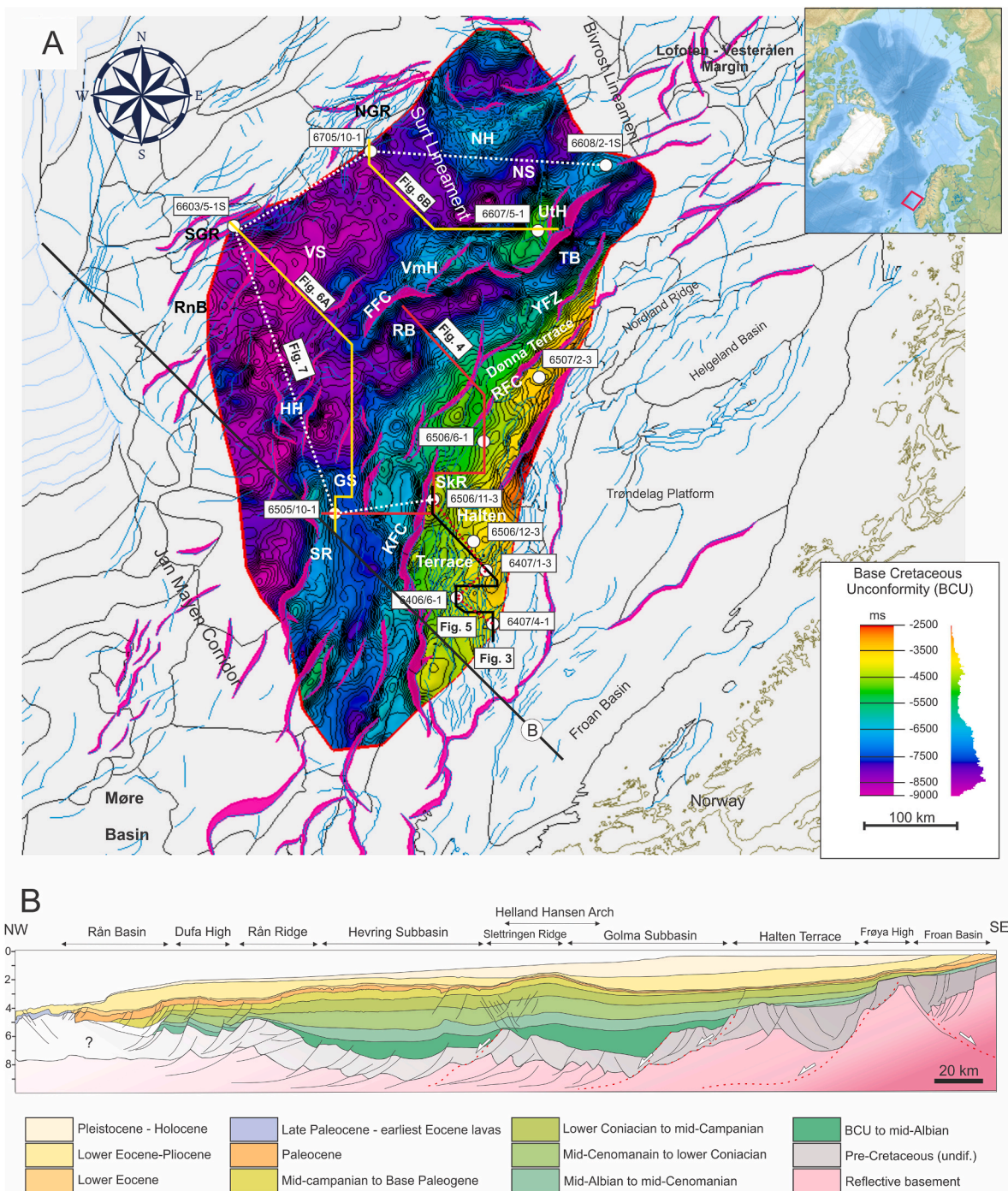


Fig. 1. (A) Time-elevation map of the Base Cretaceous Unconformity indicating the extent of the study area and outlining the main structural elements on the mid-Norwegian Margin. Wells and seismic composite lines utilized in this study are annotated. The structural elements (black lines), minor (light blue lines) and major faults (purple thick lines) are implemented after Gernigon et al. (2021). (B) Simplified geo-seismic profile outlining the structural trend and configuration of the Vøring Basin. The profile is re-drawn (with modifications) after transect “e” in Zastrozhnov et al. (2020) and is annotated “B” herein. Abbreviations after Zastrozhnov et al. (2020): SR – Slettringen Ridge, GsB – Golma Subbasin, TB – Træna Basin, VS – Vigrid Syncline, NS – Någrid Syncline, FFC – Fles Fault Complex, KFC – Klakk Fault Complex, SkR – Sklinna Ridge, SGR -South Gjallar Ridge, NGR – North Gjallar Ridge, RB – Rås Basin, RnB – Rån Basin, UtH – Utgard High, VmH – Vimur High, HH – Hevrig High, NH – Nyk High.

deposits of late Cenomanian – early Turonian age, which has been encountered in an exploration well on the Sklinna High (exploration well 6506/11–3; see NPD [Factpages, 2022, Fig. 1](#) for location). The age-equivalent organic-rich unit, the Blodøks Formation, in the North Sea, reportedly has good source rock qualities despite its thin development there ([Isaksen and Tonstad, 1989](#)). On the conjugate margin onshore East Greenland, several outcrop and shallow borehole information give hints to the presence of a potential mid-Cretaceous source rock, including oil stains in younger clastic deposits, as well as isotope and biomarker data compatible with a possible Cretaceous source rock ([Bojesen-Koefoed et al., 2020](#)). Age-equivalent organic-rich unit with source rock potential have also been documented in the Kanguk Formation within the Sverdrup Basin, and the Smoking Hills Formation in the Mackenzie Delta area, Arctic Canada ([Leith et al., 1993](#); [Lenniger et al., 2014](#); [Herrle et al., 2015](#); [Schröder-Adam et al., 2019](#)). Previous work in the Vøring Basin has also documented the occurrence of organic-rich marine mudstones in Barremian, Aptian and Albian strata ([Jongepier et al., 1996](#); [Doré et al., 1997b](#); [Wenke et al., 2021](#)). Regardless of the deep burial, it has been speculated that some of these intervals may hold some source rock potential ([Brekke et al., 1999](#)).

It is well known that the Cretaceous period experienced several short-lived Oceanic Anoxic Events (OAEs) which promoted widespread deposition of organic-rich mudstones ([Schlanger and Jenkyns, 1976](#); [Arthur and Schlanger, 1979](#); [Jenkyns, 1980](#); [Arthur et al., 1987, 1990](#); [Bralower et al., 1993](#); [Erbacher et al., 1996](#); [Midtkandal et al., 2016](#)). The two most prominent events, the OAE 1a in the early Aptian (i.e. the Selli Event) and the OAE 2 at the Cenomanian – Turonian transition (i.e. the Bonarelli Event), are both attributed to eustatically rising sea level and elevated marine productivity primed by volcanic activity and increased sea surface temperatures ([Arthur et al., 1987](#); [Erbacher et al., 1996](#); [Leckie et al., 2002](#); [Turgeon and Creaser, 2008](#); [Adams et al., 2010](#)). Source rocks associated with the OAE 2 are highly prolific and have apparently sourced a quarter of the World's petroleum ([Klemme and Ulmishek, 1991](#)).

However, because so few wells penetrate Cretaceous strata in the Vøring Basin, the distribution of potential source rocks in this interval is highly uncertain and the inferred presence of prolific Cretaceous source rocks remains speculative. In this study, we combine high-resolution regional 2D seismic data, available Rock-Eval data, and well logs, to map the distribution of and evaluate the source rock potential of several organic-rich units in the Cretaceous succession in the Vøring Basin. We particularly focus on organic-rich deposits associated with the Cenomanian/Turonian strata, and by applying traditional source rock evaluation methods (*sensu* [Peters and Cassa, 1994](#)) the potential of these deposits is meticulously assessed. We also present a depositional model for the Cenomanian – Turonian interval in the Vøring Basin, further arguing that sea-level rise and increased primary productivity during the OAE 2 coupled with extensive rifting fostered favorable conditions for organic-rich units to be deposited. Finally, we discuss our findings in relation to the tectono-sedimentary evolution of the Vøring Basin and its wider implications for the prospectivity of the mid-Norwegian margin.

2. Geological framework

2.1. Lower Cretaceous structural development

The development of the mid-Norwegian margin is related to a series of post-Caledonian rifting phases, which eventually led to the complete separation of Norway and Greenland in the Eocene ([Doré et al., 1999](#); [Brekke, 2000](#); [Tsikalas et al., 2005](#); [Lundin et al., 2013](#); [Peron-Pinvidic and Osmundsen, 2018](#); [Zastrozhnov et al., 2020](#)). The preexisting structural grain influenced the segmentation and overall geometry of the subsequent rift basins, and the conjugate margins was from early onset of rifting the fundamental source of sediments ([Rotevatn et al., 2018](#)). The Vøring Basin was formed by predominately two rifting phases during the Late Jurassic – earliest Cretaceous, and the Late Cretaceous –

Paleocene ([Blystad et al., 1995](#); [Tsikalas et al., 2005](#); [Faleide et al., 2008](#); [Zastrozhnov et al., 2020](#)). The western limit of the Vøring Basin is characterized by massive intrusive and extrusive volcanic depositions ([Peron-Pinvidic and Osmundsen, 2018](#); [Zastrozhnov et al., 2020](#)). This magmatic activity is linked to the continental breakup and started after the final rift phase in the Late Cretaceous – Paleocene ([Planke et al., 2005](#); [Abdelmalak et al., 2016](#)). The eastern limit and proximal regime of the Vøring Basin is defined by the Trøndelag Platform and the Halten and Dønna terraces ([Fig. 1](#)). The northern boundary is defined by the Jan Mayen Corridor, which separates it from the Møre Basin. Towards the north, the Vøring Basin is separated from the narrow Lofoten-Vesterålen margin by the Bivrost Lineament ([Tsikalas et al., 2019](#); [Brekke, 2000](#); [Zastrozhnov et al., 2020](#)). The Vøring Basin contains several intra-basinal highs and subbasins, reflecting a complex structural history. The most important structural elements for this study are in the necking and distal domain which are characterized by hyperextended half-grabens ([Peron-Pinvidic and Osmundsen, 2018](#); [Zastrozhnov et al., 2020](#)), and include the (Alphabetically): Gjallar Ridge, Golma Subbasin, Halten Terrace, Rås Basin, Sklinna Ridge, Træna Basin and the Vigrid Syncline ([Fig. 1](#)). A brief outline of their structural development is given below.

2.1.1. Gjallar Ridge

The Gjallar Ridge is located in the outer part of the Vøring Basin ([Fig. 1](#)) and is bounded by the Vigrid Syncline to the east and by the Fenris Graben to the west. The Gjallar Ridge consists of a series of NE trending rotated fault blocks, formed during the Late Cretaceous – Early Paleocene rift phase, prior to complete continental breakup later in the Cenozoic ([Gernigon et al., 2003](#); [Zastrozhnov et al., 2018, 2020](#)).

2.1.2. Golma Subbasin

The Golma Subbasin is a N–S trending subbasin confined between the Halten Terrace and the Slettringen Ridge ([Fig. 1](#)). Towards the north, the Golma Subbasin transitions into the Rås Basin and in the south to the Holmen Subbasin. Based on the presence of a thick Lower Cretaceous succession, the Golma Subbasin clearly acted as a prominent depocenter during Early Cretaceous times ([Zastrozhnov et al., 2020](#)).

2.1.3. Halten Terrace

The Halten Terrace is a faulted terrace transitionally located between the Trøndelag Platform in the east and the Rås Basin in the west ([Fig. 1](#)). The terrace is c. 80 km wide and c. 130 km long, bounded by fault complexes along all its margins (e.g. [Blystad et al., 1995](#); [Hansen et al., 2021](#); [Bell et al., 2014](#); [Gernigon et al., 2021](#)). Its formation involves multiple extensional phases during the Palaeozoic, Mesozoic and earliest Cenozoic ([Blystad et al., 1995](#); [Doré et al., 1997a](#); [Hansen et al., 2021](#)). The main structural shaping is attributed to the Late Jurassic to Early rifting phase which formed several fault-bound depocenters, that eventually joined into a single depocenter in the Late Cretaceous (e.g. [Bell et al., 2014](#)). The Halten Terrace includes a Lower to Upper Cretaceous succession (c. 0.8 S TWT thick, including Cenomanian deposits) which is markedly thinner than the equivalent stratal succession in the Vøring Basin, yet thicker and more complete than the condensed and commonly eroded stratal package sitting on the platform domain further to the east. Deep marine conditions prevailed during deposition of Lower to Upper Cretaceous sediments ([Blystad et al., 1995](#); [Doré et al., 1997a](#); [Hansen et al., 2021](#)). These sediments were predominantly sourced from regional highs (e.g. Sklinna High and Frøya High) and the Trøndelag Platform which separated from the Halten Terrace in the Late Cretaceous ([Blystad et al., 1995](#); [Brekke et al., 2001](#)).

2.1.4. Rås Basin

The Rås Basin is delimited to the east by the Halten and Dønna Terraces, separating them are the Klakk and Ytreholem Fault Complexes ([Blystad et al., 1995](#); [Zastrozhnov et al., 2020](#)). The Fles Fault Complex separates the Rås Basin from the Vigrid Syncline in the west, while the southern and northeastern boundaries are defined by the Jan Mayen and

Surt Lineaments. (Blystad et al., 1995). The Rås Basin contains thick Cretaceous deposits where the greatest thickness (c. 5 S TWT) is reported along the central axis of the basin (Blystad et al., 1995). As such, the basin was a major depocenter for sediments throughout the Cretaceous period (Zastrozhnov et al., 2020).

2.1.5. Sklinna Ridge

The Sklinna Ridge is located on the western margin of the Halten Terrace (Fig. 1). The N-S elongated ridge is c. 140 km long and 13 km wide. The Sklinna Ridge was formed due to uplift along the Klakk Fault Complex during the Late Jurassic – Early Cretaceous rifting event (Blystad et al., 1995). Consequently, the top of the ridge has been subject to erosion since its formation and has been a local sediment source for Lower to Upper Cretaceous sediments (Blystad et al., 1995; Bell et al., 2014; Hansen et al., 2021). Internally, the ridge has a complex fault pattern with a series of intersecting N-S- and NE-SW-striking faults (Blystad et al., 1995).

2.1.6. Træna Basin

The Træna Basin is an elongated NE-SW oriented feature in the northeastern part of the Vøring Basin. It is bounded in the east by the Ytreholmen Fault Zone along the Dønna Terrace in the south and the Revallet Fault Complex along the Nordland Ridge to the north (Fig. 1; Blystad et al., 1995). The western flank is defined by the Fles Fault Complex which bounds the Utgard High. To the south and north the basin is delimited by the Surt and Bivrost lineaments, respectively. The Træna Basin was formed by Late Jurassic – Early Cretaceous crustal extension and faulting, subsequently undergoing significant thermal subsidence. (Blystad et al., 1995; Zastrozhnov et al., 2020). Consequently, the basin contains deeply buried Lower Cretaceous sediments. The Træna Basin was also a prominent depocenter during the Late Cretaceous (Zastrozhnov et al., 2020).

2.1.7. Vigrid Syncline

The Vigrid Syncline is oriented NE-SW and is bounded by the Gjallar Ridge to the west, the Fles Fault Complex to the east, the Surt Lineament to the north and the Jan Mayen Lineament to the south (Fig. 1). Much of the strata in the Vigrid Syncline is made up of Upper Cretaceous

deposits, with thicknesses reaching c. 4.5 S TWT, albeit significantly thinning along the western flank (Blystad et al., 1995). Based on the occurrence of Lower Cretaceous strata, the Vigrid Syncline also acted as a depocenter during the Early Cretaceous (Zastrozhnov et al., 2020).

2.2. Lower Cretaceous stratigraphy

The Lower Cretaceous succession on the mid-Norwegian Continental margin has traditionally been divided into the Lyr (Late Berriasian – Early Aptian), Lange (Berriasian – Turonian) and Lysing (Latest Turonian – Early Coniacian) Formations, collectively assigned to the Cromer Knoll Group (Dalland et al., 1988). Recently, however, the original Lange Formation, as defined by Dalland et al. (1988), has been sub-divided into the Langebarn (Berriasian – Late Albian) and the Blålange Formations (Early Cenomanian – earliest Coniacian) (Fig. 2A) cf. Gradstein et al. (2010). Concomitantly, the Blålange Formation has been re-assigned to the Shetland Group, and the renowned turbidite sandstone-dominated Lysing is now ranked as a member of the Blålange Formation (Gradstein et al., 2010) The Lyr and Langebarn Formations are retained within the Cromer Knoll Group (Fig. 2).

The base of the Cretaceous succession is defined by the regional extensive erosive boundary, referred to as the Base Cretaceous Unconformity (BCU) (e.g. Færseth and Lien, 2002; Faleide et al., 2015).

The 0.5–444 m thick Lyr Formation (Late Berriasian -early Aptian) was deposited under open marine conditions and consists of grey to light grey-green marls with interbedded carbonates (Dalland et al., 1988; Gradstein et al., 2010). The Lyr Formation is regionally extensive and stretch across from the Trøndelag Platform to the Halten Terrace. but the unit is eroded or extremely condensed on the Nordland Ridge and has not been penetrated by any exploration wells further west in the Vøring Basin, suggesting that the unit represents a shallow shelf deposit. The upper part of the formation may show a sharp gamma ray response, that may be attributed to the presence of lower Aptian organic-rich mudstones deposited under the OAE1a. See NPDP Factpages (2022) for type and reference wells (i.e. 6506/12-1 and 6407/1-2).

The overlying Langebarn Formation (Berriasian – Late Albian) is 3–467 m thick and consists mainly of marine mudstones with some limestone stringers and occasional sandstone units (Dalland et al., 1988;

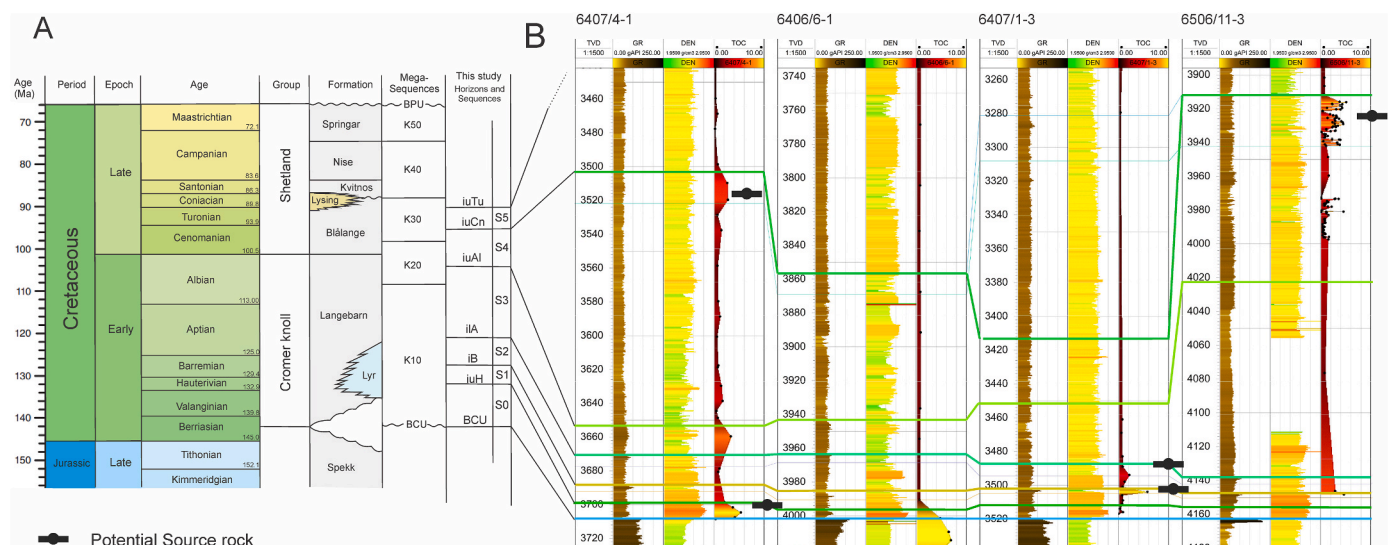


Fig. 2. (A) Lithostratigraphic overview of the Lower Cretaceous succession on the mid-Norwegian Margin. The succession has been subdivided into a series of mega-sequences by Færseth and Lien (2002). The Chronostratigraphic chart has been modified after Cohen et al. (2013). The interpreted seismic horizons and sequences are annotated. B) Well correlation of four selected wells situated on the south-western margin of the Halten Terrace, showing the presence of four organic-rich units with high GR and TOC values: (1) an upper Hauterivian unit in well 6407/4-1, (2) a Barremian unit in well 6407/1-3 (3) a lower Aptian unit well 6407/1-3 and (4) an upper Cenomanian potential source rock unit in well 6506/11-3 and partly in 6407/4-1. Abbreviations: iuCn: intra upper Cenomanian reflector, iuAl: Intra upper Albian reflector, iIA: intra lower Aptian reflector, iB: intra Barremian reflector, iuH: intra upper Hauterivian reflector, BCU: Base Cretaceous Unconformity, BPU: Base Paleogene Unconformity, GR: Gamma ray log, DEN: Density log, TOC: Total organic carbon (wt. %).

Gradstein et al., 2010). The formation was deposited in shallow to deep marine environments (Dalland et al., 1988; Gradstein et al., 2010). The Langebarn Formation is laterally extending across the Halten and Dønna terraces and the basinal area but is eroded on the Nordland Ridge.

The up to 1573 m thick (well 6505/10–1) Blåånge Formation (Early Cenomanian – earliest Coniacian) consists predominantly of dark grey to brown mudstones with limestone stringers, but locally include several tens of meters thick turbidite sandstone units (such as the Lysing Member sandstones) which accumulated in isolated fault-bound basins on the Halten and Dønna terraces and along the Møre margin (e.g. Vergara et al., 2001; Fjellanger et al., 2005; Martinsen et al., 2005; Gradstein et al., 2010; Bell et al., 2014). Most of the mudstones of the Blåånge Formation was deposited in a relatively deep, restricted marine environment strongly influenced by the rift-related bathymetry of the region and the limited connection between the various basins of the North Atlantic rift system (Gradstein et al., 1999). Due to limited water circulation, a stratified water column and widespread oxygen deficient bottom water conditions developed. The potential upper Cenomanian–lower Turonian source rock unit investigated in this paper occur within the Blåånge Formation (Fig. 2).

3. Data and methods

3.1. Seismic data

Several high-resolution 2D seismic surveys (MNR 2004–2011) have been analyzed to establish and map the seismic horizons used to investigate the organic-rich units in the Cretaceous succession of the Vøring Basin. These surveys have different orientation and variable spacing between seismic lines, ranging from 1 to 8 km. Frequencies typically range between 10 and 50 Hz. The polarity convention for the dataset is zero-phase, normal polarity (*sensu* Sheriff, 2002).

In the Vøring Basin, most of the Lower Cretaceous succession is deeply buried down to depths of 6–9 S TWT, thus confidence in seismic interpretation and reflector correlation towards the deeper segments is strongly affected by decreasing seismic quality with depth. However, the overall quality of the seismic data is good, although there are some noticeable differences between the surveys.

3.1.1. Mapping of potential source rock units

A total of seven seismic horizons of regional to semi-regional extent have been defined and mapped in this study (Fig. 2). These includes the Base Cretaceous Unconformity (BCU; *sensu* Færseth and Lien, 2002), the intra upper Albian (iuAl) and the intra upper Cenomanian horizon (iuCn), which have been interpreted on regional scale and further tied to key wells in the outer Vøring Basin. In addition, the intra upper Hauterivian (iuH), intra Barremian (iB), intra lower Aptian (iLA), and intra upper Turonian (iuTu) seismic horizons have been interpreted at semi-regional scale on the Dønna and Halten terraces. These horizons are not correlated towards the deeper basin segments due to the lack of well data, diminishing seismic quality and the corresponding uncertainty in tracing these reflectors basinwards. In addition, any organic matter associated with these horizons would presumably be classified as overmature in the deeper basin segments. For this reason, these units are treated superficially throughout the remaining part of the paper.

Age determination of the mapped seismic horizons are guided by the works of Gradstein et al. (2010) and Zastozhnev et al. (2020), together with well tops from the publicly available database of the Norwegian Petroleum Directorate (NPD Factpages, 2022) and in-house data provided by Wintershall-Dea Norway.

3.2. Well data

Wireline data from 12 exploration wells are included in this study, each dataset including Gamma ray (GR), Acoustic (AC/DT), Density (DEN), Neutron (NEU) and deep resistivity (RDEP) logs. We have

established the time-depth relationship through calibration of checkshots. Wireline logs are generally regarded to be a good supplement to seismic data when evaluating the presence of potential source rock units (Løseth et al., 2011; Hagset et al., 2022). As such, to confirm the presence of potential source rock units mapped in the seismic data, wireline log signals are integrated with digitalized total organic carbon (TOC) content logs derived from the Rock-Eval data. The thicknesses of the potential source rock units are estimated from the wireline data and subsequently, TOC samples within the interval, or from stratigraphically nearby intervals, are evaluated. Characteristic wireline responses to organic rich units are described in Hagset et al. (2022).

3.3. Rock-Eval data and interpretation

The Rock-Eval database is based on samples from sidewall cores or drill cuttings from 12 exploration wells. The database is thus based on results from previous geochemical analysis. Data quality control has been conducted to ensure that abnormal values are excluded. Unfortunately, some of the samples are missing values for the oxygen index (OI). In addition, sample spacing varies between each well, making it difficult to evaluate thin, intervening organic-rich deposits. In these cases, the nearest sample to the organic-rich unit have been used where applicable. The Rock-Eval database has been implemented into a Petrel project, making it possible to evaluate the link between seismic character, wireline logs and Rock-Eval data. This also help identify organic-rich units during well correlation and in the seismic section (e.g. Hagset et al., 2022). The complete Rock-Eval database is provided in the online supplementary file SF1.

This study applies traditional source rock evaluation following the principles of Espitalié et al. (1977), Peters (1986) and Peters and Cassa (1994) in order establish the type, richness, and thermal maturity of the organic-rich units. The thermal maturity has been established using T_{max} values, because there are no vitrinite reflectance (R_o) data available.

4. Results

4.1. Lower Cretaceous seismic sequences and bounding surfaces

Six genetic sequences (S0 – S5) and their corresponding bounding surfaces (i.e. the BCU, iuH, iB, iLA, iuAl, iuCn, iuTu reflectors of this study) have been recognized and interpreted in the Lower to lowermost Upper Cretaceous succession in the Vøring Basin (Figs. 3 and 4). Apart from the Base Cretaceous Unconformity (BCU), which defines the base of the Lower Cretaceous succession, and the unconformity related to the iuCn reflector on the Halten Terrace, the sequence-bounding surfaces presumably represent maximum flooding surfaces. Below follows a description of the seismic characteristics of each genetic sequence and their bounding surfaces.

4.1.1. Sequence 0 (Berriasian – Hauterivian)

Sequence 0 is bounded at the base by the BCU and at the top by the intra upper Hauterivian reflector (iuH). The BCU defines the base of the Lower Cretaceous succession and is characterized by a continuous and prominent seismic acoustic impedance contrast. The BCU is regional extensive and can be interpreted with high confidence. The iuH reflector has a variable continuity and negative amplitude character. Sequence 0 is deeply buried in the Vøring Basin and severely condensed on the Halten and Dønna terraces (Fig. 3). Internally, Sequence 0 has a sub-parallel reflection configuration, where reflectors appear semi-coherent with low to medium amplitudes.

4.1.2. Sequence 1 (Hauterivian – early Barremian)

Sequence 1 is bounded at the base by the iuH reflector and at the top by the intra Barremian reflector (iB). The iB reflector is discontinuous and has a weak negative amplitude. Sequence 1 is present on the Halten Terrace in downfaulted sections and towards the western margin of the

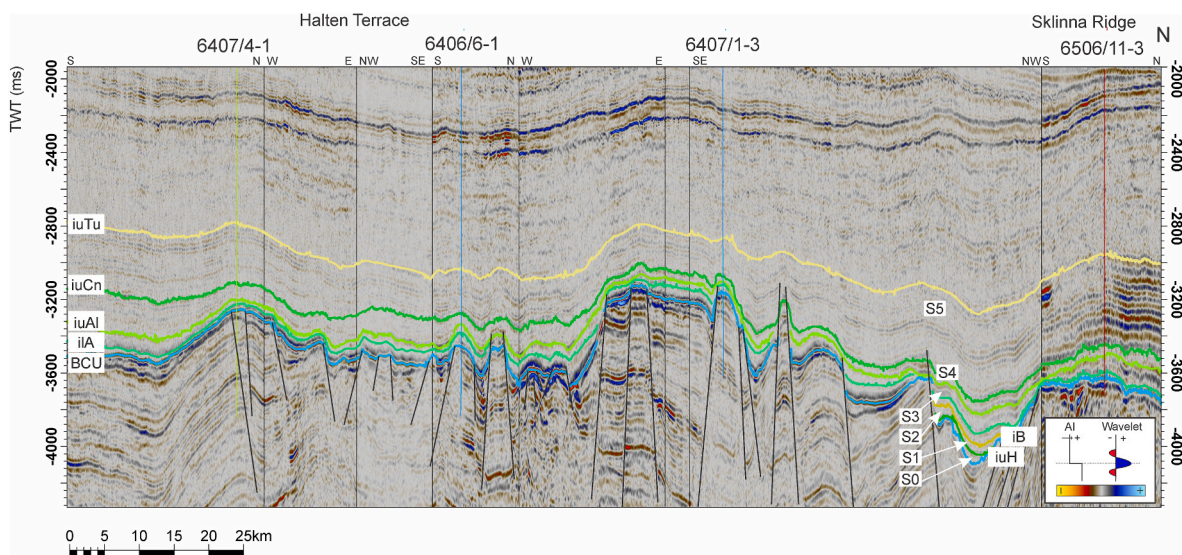


Fig. 3. Composite seismic profile crossing the southern Halten Terrace, displaying the stratigraphic framework of the condensed Lower Cretaceous succession with the sequences of this study indicated (S0–S6). The seismic has been tied to wells 6407/4–1, 6406/6–1, 6407/1–3 and 6506/11–3. The corresponding well-correlation is shown in Fig. 5, whereas location of the composite seismic profile and wells is shown in Fig. 1. Abbreviations for seismic reflectors: iuTu: intra upper Turonian, iuCn: intra upper Cenomanian, iuAl: intra upper Albian, ilA: intra lower Aptian, iB: intra Barremian, iuH: intra upper Hauterivian.

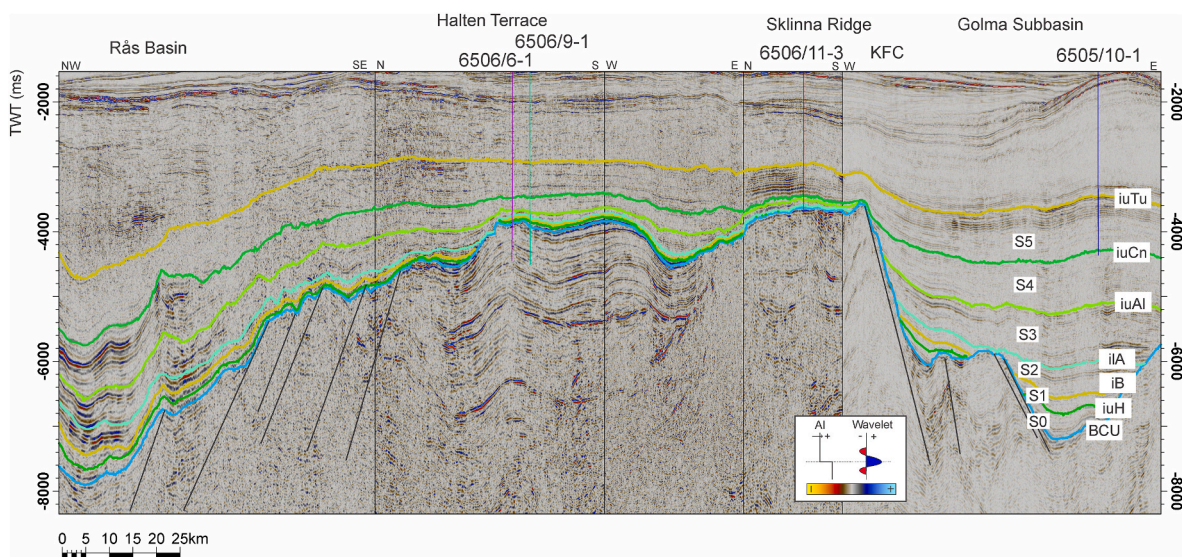


Fig. 4. Composite seismic line crossing the Træna Basin, Halten Terrace, Sklinna Ridge and Rås Basin. The seismic profile is displaying the stratigraphic framework of the Lower Cretaceous succession. Wells 6506/6–1, 6506/9–1, 6506/11–3 and 6505/10–1 are tied to the seismic. Note the deep position and lack of well control of the Lower Cretaceous horizons in the Træna and Rås Basins. Location of the composite seismic profile and wells is shown in Fig. 1. Abbreviations: iuTu: intra upper Turonian, iuCn: intra upper Cenomanian, iuAl: intra upper Albian, ilA: intra lower Aptian, iB: intra Barremian, iuH: intra upper Hauterivian, KFC: Klakk Fault Complex.

terrace (Fig. 3). The sequence is strongly condensed and has semi-coherent, subparallel reflectors with low amplitude characteristics.

4.1.3. Sequence 2 (Barremian – Early Aptian)

Sequence 2 is bounded at the base by the iB reflector and at the top by the intra lower Aptian reflector (ilA). The ilA reflector is continuous over the Halten Terrace and is characterized by low amplitudes (Fig. 3). Locally, sequence 2 is strongly condensed and the ilA reflector is obscured in places. Sequence 2 has a semi-coherent subparallel reflection configuration on the Halten Terrace, highly affected by erosion or non-deposition (Fig. 3).

4.1.4. Sequence 3 (Early Aptian – Late Albian)

Sequence 3 is bounded at the base by the ilA reflector and at top by the intra upper Albian reflector (iuAl). The iuAl reflector has a medium negative amplitude and is continuous across the Halten Terrace and can be traced into the Rås and Træna basins (Fig. 3). The internal reflection configuration of sequence 3 show parallel to subparallel reflectors, which has a low to medium amplitude. These reflectors are discontinuous and have low amplitudes within the deeper segments of the Rås and Træna basins (Fig. 4).

4.1.5. Sequence 4 (Late Albian – latest cenomanian)

Sequence 4 is bounded at the base by the iuAl reflector and at top by the iuCn reflector. The iuCn seismic reflector is continuous with low –

medium amplitude characteristics. The reflector is regionally distributed on the mid-Norwegian margin and penetrated by most of the wells on the Halten Terrace. Internally, Sequence 4 show subparallel discontinuous reflectors with low-medium amplitude characteristics.

4.1.6. Sequence 5 (latest cenomanian – late turonian)

Sequence 5 is bounded at the base by the iuCn reflector and atop by the iuTu reflector. The iuTu reflector has a negative amplitude and appear continuous on the Halten Terrace. The reflector, which marks the end of the Turonian stage, can be interpreted with high confidence across the Vøring Basin. Internally, sequence 5 has subparallel semi-coherent reflectors with variable amplitude characteristics (Fig. 3).

4.2. Potential Lower Cretaceous source rock units

Five negative reflectors have been recognized and mapped in the study area. These are the: i) intra upper Hauterivian (iuH), ii) intra Barremian (iB), iii) intra lower Aptian (ilA), iv) intra upper Albian (iuAl), and v) the intra upper Cenomanian (iuCn) reflectors. These reflectors correlate to wireline signals and raised TOC contents in several of the key exploration wells (Fig. 5; Table 1), presumably indicating the presence of organic-rich units (Løseth et al., 2011; Hagset et al., 2022).

The Lower Cretaceous organic-rich units, in particular those associated with the iB, ilA, and iuAl reflectors, are present on the Halten Terrace, as evident by increased TOC and S2 values in wells 6407/4–1, 6406/6–1, 6407/1–3 and 6506/11–3 (Fig. 5). However, it is generally difficult to tie the wireline signals of these units to distinct reflectors as the thickness of the individual units appear to be below seismic resolution. Occasionally, some of the related reflectors can be recognized in downfaulted blocks on or along the margin of the terrace (Figs. 3 and 4). Nonetheless, due to limited well-control, variable seismic quality and resolution, complex fault geometries, and great burial (i.e. 6–8 s TWT), all the reflectors which possibly relate to Lower Cretaceous organic-rich units are difficult to identify and confidently tie to the deeper basinal segments of the mid-Norwegian margin (Fig. 4). Although the thickness and potential of these units may be greater in the adjacent Rås and Træna basins (Fig. 4), we will focus on the organic-rich unit corresponding to the upper Cenomanian reflector in the remaining part of this paper. A detailed description of this organic-rich unit is given below, whereas the sampled intervals, typical wireline signals, TOC contents, and Rock-Eval parameter S2 is summarized in Table 1.

4.2.1. The intra upper cenomanian reflector

4.2.1.1. Lateral distribution and seismic characteristics.

The iuCn reflector is traceable across the Halten Terrace and generally appears as a continuous reflector of low to medium negative amplitudes (Fig. 3). Albeit amplitude characteristics can change laterally, the reflector remains coherent over most of the Halten Terrace and the Sklinna Ridge. Towards the southwestern margin of the Halten Terrace, the iuCn reflector is downfaulted along the Klakk Fault Complex into the Golma Subbasin (Fig. 4), where the reflector remains continuous with low to medium negative amplitudes. The iuCn reflector is tied to well 6505/10–1 in the Golma Subbasin (see iuCn and well 6505/10–1; Fig. 4). From this location, the reflector can be traced laterally over the Slettringen Ridge, paralleling the Klakk Fault Complex further into the Rås and Træna Basins.

In the Rås Basin, the iuCn reflector has the same configuration with continuous low to medium negative amplitudes (Figs. 4 and 6A) Towards the more distal domain, the iuCn reflector can be traced past the Fles Fault Complex and into the deeper Vigrid Syncline (Fig. 6A). Here, the reflector remains coherent with low to medium negative amplitude, only segmented by minor down-faulting and doming. The reflector overlies the uplifted Gjallar Ridge, where the reflector is penetrated by well 6603/5-1 S (Fig. 6A).

The iuCn reflector can also be mapped and traced along the Vigrid Syncline, where it is correlated to well 6705/10-1 situated at the margins of the northern part of the Gjallar Ridge and well 6607/5-1 located at the Utgard High (Fig. 6B). At this location, in the deeper parts of the Vigrid Syncline, the iuCn reflector have low – medium negative amplitudes and appear semi-coherent (Fig. 6B).

4.2.1.2. Well correlation.

Fig. 5 shows a well correlation panel from the southern parts of the Halten Terrace and Sklinna Ridge. Here, the iuCn reflector corresponds to the top of an interval exhibiting increased TOC contents and S2 values in wells 6407/4–1, 6407/1–3 and 6506/11–3 (Fig. 5). Concomitantly, wireline logs indicate slightly increased GR and RDEP values in response to the raised TOC content in well 6506/11–3 (Fig. 5). In contrast, wireline logs in well 6407/1–3 and 6407/4-1 do not show any significant response to the increased TOC content (Fig. 5). Increased TOC and S2 levels are also recorded in well 6507/2–3 situated near the Dønna Terrace (Fig. 1 and Table 1).

The correlation panel shown in Fig. 7 includes exploration wells

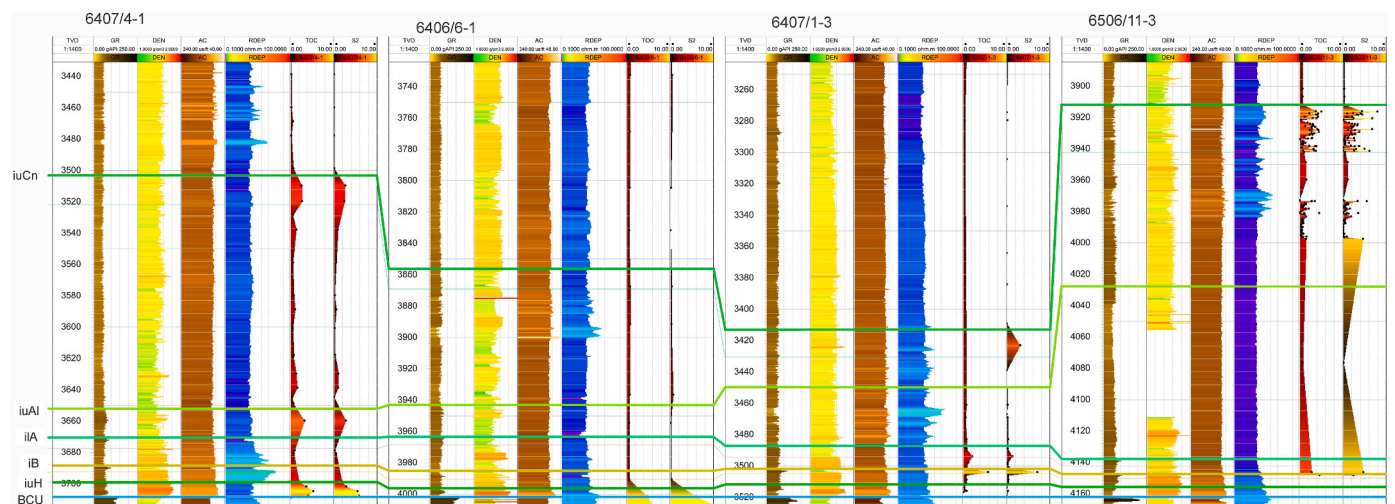


Fig. 5. Correlation of wells 6407/4–1, 6406/6–1, 6407/1–3 and 6506/11–3 on the Halten Terrace and Sklinna Ridge. The seismic reflectors mapped in this study is annotated, including the BCU (Base Cretaceous unconformity), iuH (intra upper Hauterivian), iB (intra Barremian), ilA (intra lower Aptian), iuAl (intra upper Albian) and iuCn (intra upper Cenomanian). Abbreviations: GR: Gamma ray, DEN: Density, AC: Acoustic/Sonic, RDEP: Deep Resistivity, TOC: Total Organic Carbon, S2: Rock-Eval “S2” parameter. Scaling and color schemes are indicated. The Black points along the TOC and S2 log are sample points. Location of wells is indicated in Fig. 1.

Table 1

Interval, wireline log and Rock-Eval values for the upper Cenomanian organic-rich unit in key exploration wells situated on the Halten Terrace and elsewhere in the Vøring Basin. Average values are given in brackets. Single values indicate one sample point for the interval. Rock-Eval values in well 6603/5-1 S are taken close to the sample interval.

Well	Interval (m)	GR (gAPI)	DEN g/cm ³	AC (us/ft)	RDEP (ohm.m)	TOC (Wt %)	S2 (mg/g)
6407/4-1	3503–3521	40–60	2.4–2.6	95–105	1.1–1.6	2.66–2.78 (2.72)	2.46–2.69 (2.58)
6406/6-1	3856–3868	55–70	2.2–2.6	80–95	1.25–1.7	0.84	0.43
6407/1-3	3412–3430	45–70	2.75–2.43	85–105	1.47–4.8	None in interval: 0.8	3.11
6506/6-1	3797–3833	44–85	2.5–2.92	80–100	1.65–2.75	0.68–3.83 (1.83)	0.29–5.13 (2.36)
6506/12-3	3563–3595	35–67	2.3–2.53	78–105	1.29–2.83	0.79–1.86 (1.14)	0.23–13.08 (3.58)
6507/2-3	3253–3263	N/A	2.29–2.56	83–102	1.85–3.32	0.75–11.88 (2.30)	1.12–28.06 (4.11)
6607/5-1	3653–3693	85–250*	2.33–5.7	94–105	1.0–2.2	0.18–0.75 (0.56)	0.06–0.72 (0.41)
6506/11-3	3912–3942	30–75	2.3–2.75	80–110	1.0–6.1	0.19–5.07 (2.53)	0.03–7.89 (2.30)
6505/10-1	4940–4964	80–100	N/A	98–61	1.78–5.5	1.20–1.50 (1.35)	3.08
6603/5-1 S	3825–3848	98–85	2.60–2.70	84–93	2.2–2.85	0.89–1.00 (0.94)	1.24–1.28 (1.26)
6705/10-1	3603–3621	82–95	2.3–2.5	N/A	2.5–3.4	1.97	5.82
6608/2-1 S	3882–2998	80–145	2.4–2.75	80–95	1.6–3.9	N/A	N/A

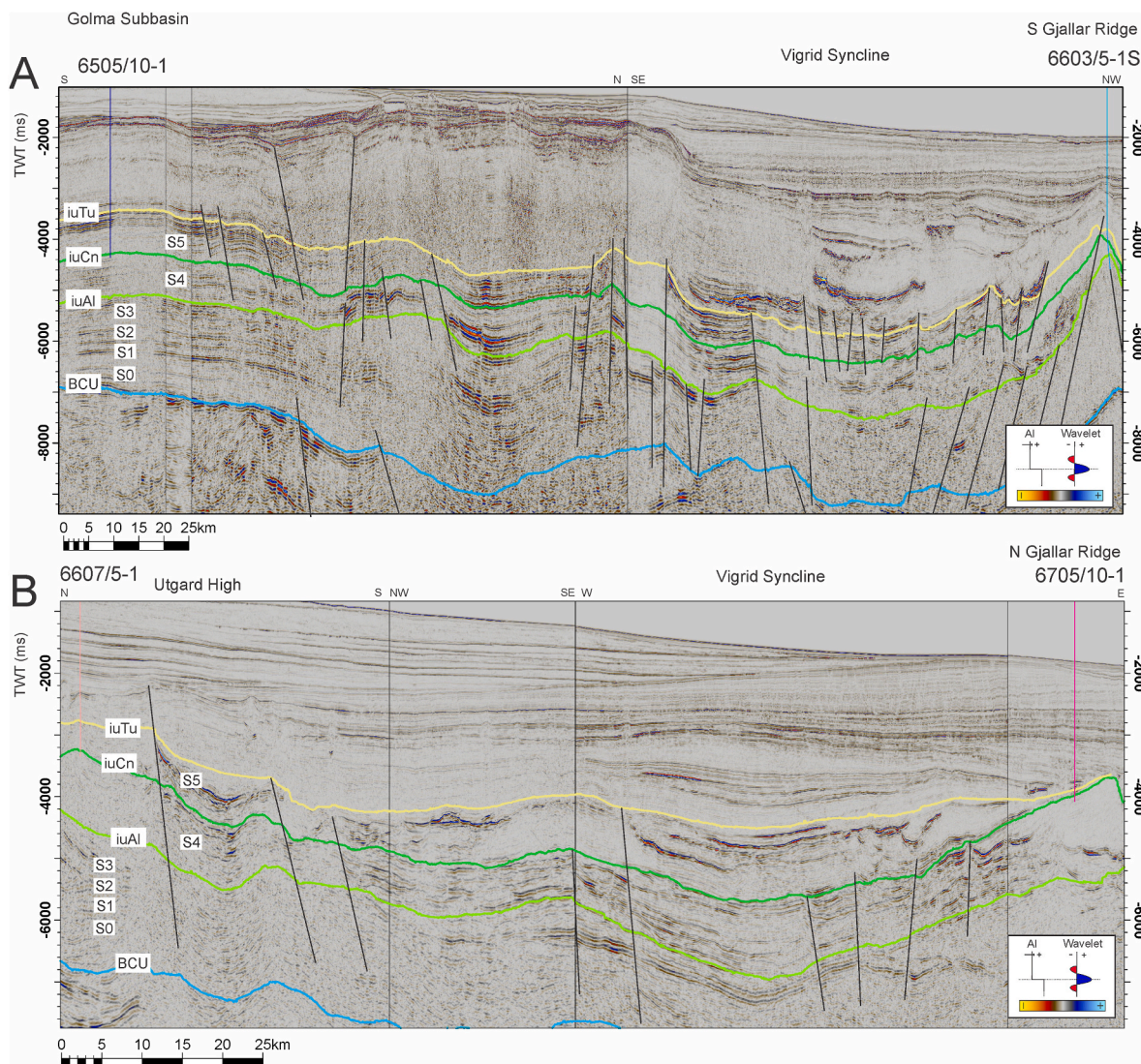


Fig. 6. Composite seismic lines crossing the outer part of the Vøring Basin. (A) Composite seismic section indicating the correlation between well 6505/10-1 in the Golma Subbasin and well 6603/5-1 S at the southern part of the Gjallar Ridge. (B) Seismic composite line displaying the correlation between well 6607/5-1 at the Utgard High and well 6705/10-1 at the northern section of the Gjallar Ridge. Seismic reflectors and sequences are annotated. Location and orientation of the composite lines is indicated in Fig. 1. Abbreviations: iuTu: intra upper Turonian, iuCn: intra upper Cenomanian, iuAl: intra upper Albian, ilA: intra lower Aptian, iB: intra Barremian, iuH: intra upper Hauterivian.

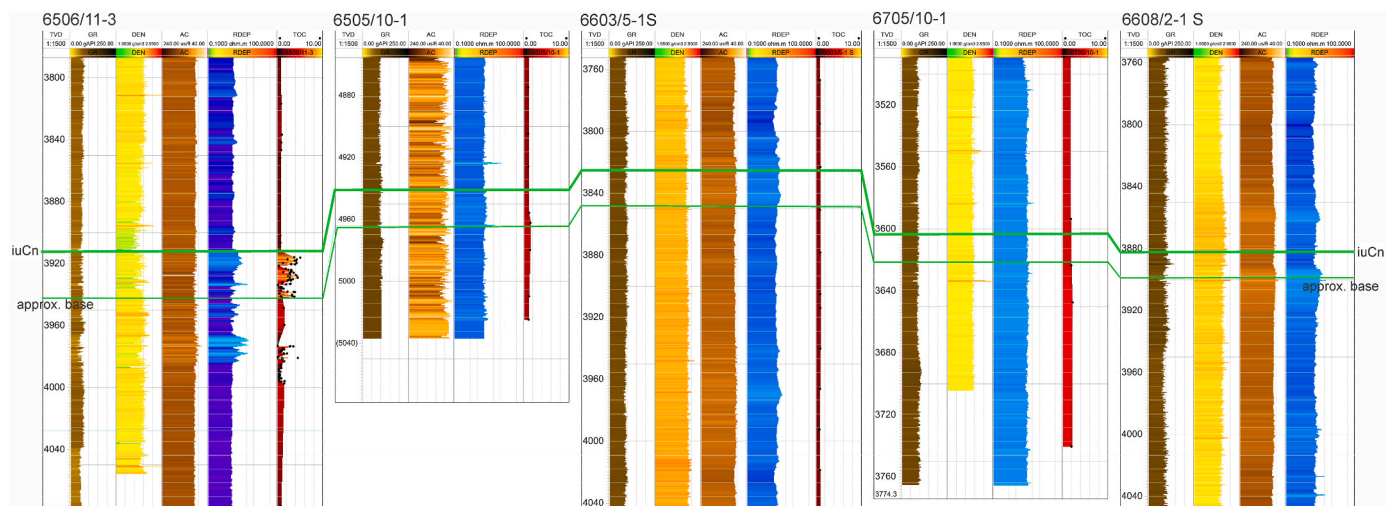


Fig. 7. Correlation of wells 6506/11-3, 6505/10-1, 6603/5-1 S, 6705/10-1 and 6608/2-1 S demonstrating the extent and character of the iuCn reflector (intra upper Cenomanian) and the base of the associated organic-rich unit. Location of wells is indicated in Fig. 1. Abbreviations: GR: Gamma ray, DEN: Density, AC: Acoustic/Sonic, RDEP: Deep Resistivity, TOC: Total Organic Carbon. S2: Rock-Eval “S2” parameter. Scaling and color schemes are indicated. The Black points along the TOC and S2 log are sample points.

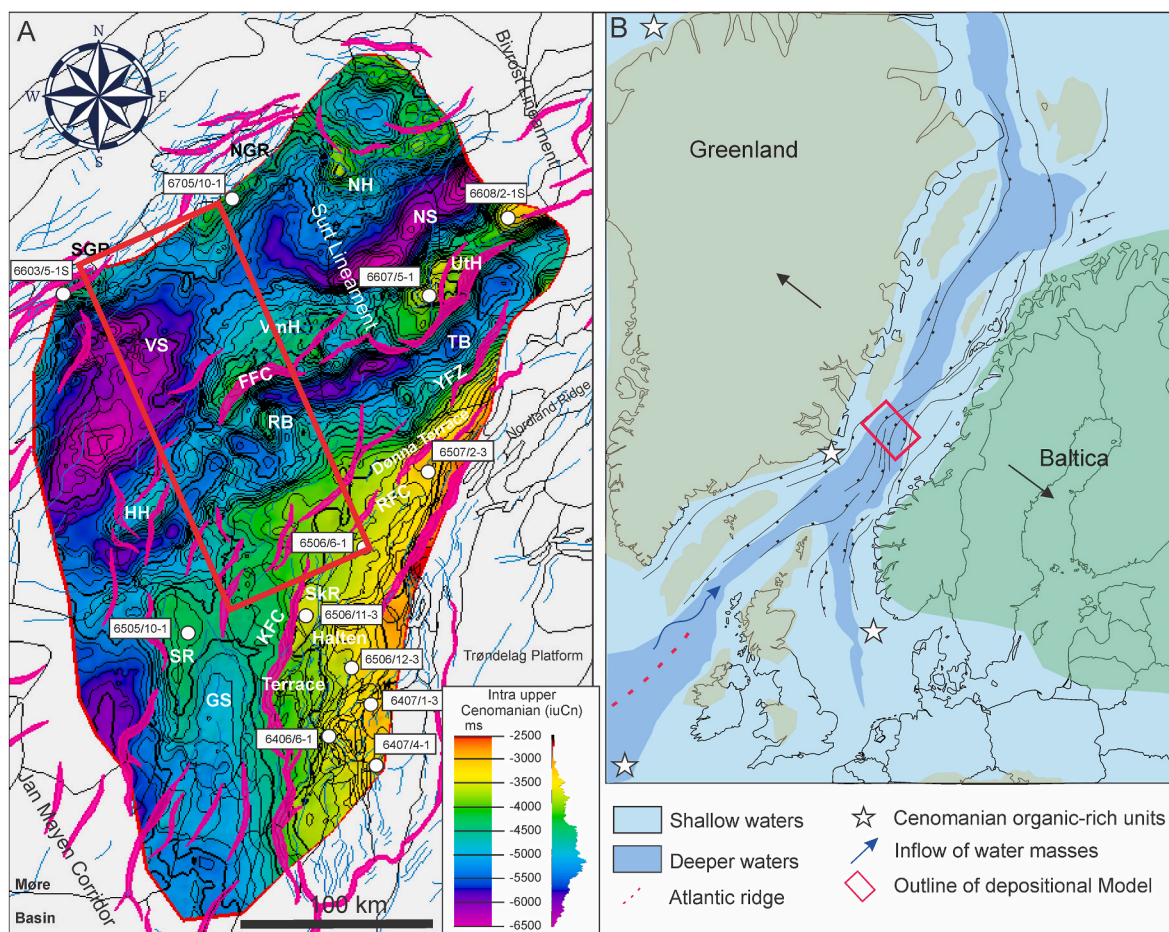


Fig. 8. (A) Time-elevation map of the intra upper Cenomanian reflector (iuCn). The structural elements (black lines), minor (light blue lines) and major faults (purple thick lines) are implemented after Gernigon et al. (2021). Color-scale with value distribution is indicated. Exploration wells of this study are indicated. (B) Paleogeographic map of the mid-Norwegian margin and north Atlantic during the Cenomanian. The map is re-drawn after Gradstein et al. (1999) and include (with modification) some of the major faults in Faleide et al. (2008) The approximated extent of the depositional model presented in Fig. 10 is indicated on the map. The presence of Upper Cenomanian organic-rich units documented in the North Sea, Sverdrup Basin and the NE Greenland is also indicated, after Doré et al. (1997b).

6506/11-3, 6505/10-1, 6603/5-1 S, 6705/10-1 and 6608/2-1 S and document the extent and character of the iuCn reflector. The three latter wells are tied to the iuCn reflector in the outer part of the Vøring Basin. Particularly well 6505/10-1 gives an unequivocal confirmation of the stratigraphic position of the iuCn reflector in a deep basinal setting in the Golma Subbasin west of the Halten Terrace. Common to these outer basin-positioned exploration wells (i.e. 6505/10-1, 66035-1 S, 6705/10-1 and 6608/2-1 S) is the absence of increased TOC values and wireline responses associated with the iuCn reflector (Fig. 7).

4.2.1.3. *Evaluation and regional interpretation.* A time-elevation map has been generated for the iuCn reflector based on interpretation of the regional 2D seismic data and the well correlations (Fig. 8). The time-elevation map reveals that the iuCn reflector generally parallel the underlying structural elements, albeit commonly being delimited by structural highs (Fig. 8). This is also documented by the onlapping nature of the reflector against for example the Sklinna Ridge and the marked thinning of Sequence 5 onto and across the Halten Terrace (Figs. 4 and 6). As such, the well correlation and regional seismic interpretation, document that the iuCn reflector is laterally extensive

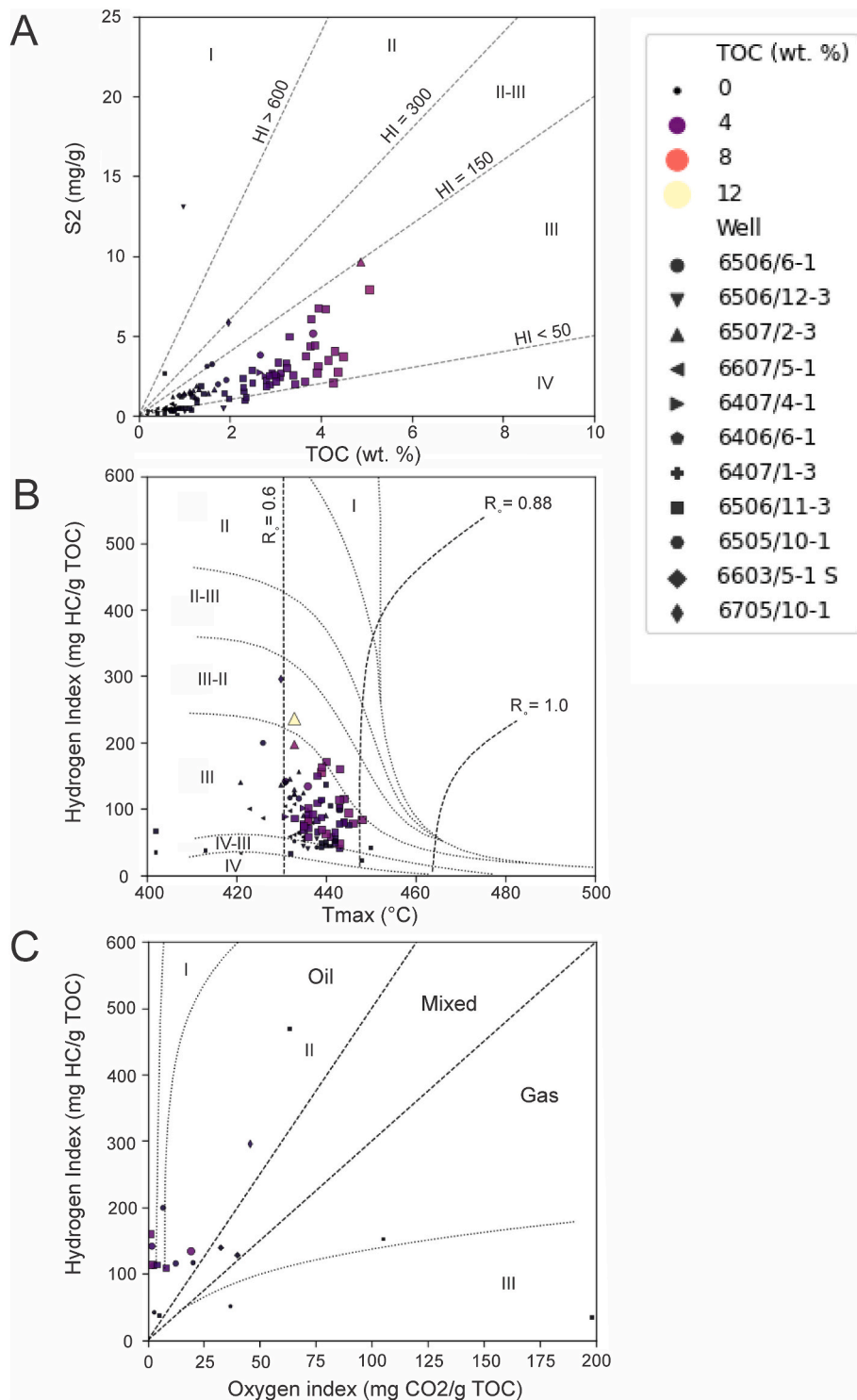


Fig. 9. Diagrams documenting the potential of the upper Cenomanian source rock unit (Corresponding to the iuCn reflector) in key wells on the mid-Norwegian Margin. The sample points increase in size depending on TOC values. Each well have a specific marker. The sample interval and thickness is shown in Table 1. Location of exploration wells is indicated in Fig. 1 (A) TOC content plotted against Rock-Eval S2 values. Kerogen type indicators are overlying the cross plot as Hydrogen index (HI) lines. (B) plot of T_{max} vs. HI indicating the petroleum potential and maturity of the samples. Overlying are the vitrinite reflectance (R_o) lines after Isaksen and Ledje (2001). (C) van Krevelen diagram of HI vs. OI indicating the quality and maturation level of the samples. Unfortunately, very few OI datapoints are available.

over large parts of the Vøring Basin.

Based on the negative amplitude of the reflector, affirmative wireline log responses, increased TOC contents and S2 values, the iuCn reflector is interpreted to represent a potential upper Cenomanian source rock unit on the Halten Terrace, Sklinna Ridge and possibly the adjacent Golma Subbasin, Rås and Træna basins (Figs. 3–5). Similar positive correlations between seismic, wireline and TOC data has been used to infer source rock units elsewhere (e.g. Løseth et al., 2011; Marín et al., 2020; Hagset et al., 2022) However, in the outer Vøring Basin, the localized lack of corresponding wireline responses and variable TOC contents (see wells 6505/10–1, 6603/5-1 S, 6705/10–1 and 6608/2-1 S; Figs. 6 and 7) related to the iuCn reflector, indicates a rather patchy distribution for the upper Cenomanian source rock unit. Consequently, it is problematic to fully assess the unit's regional potential and confidently include it in exploration models. Despite these uncertainties, we evaluate the potential of the upper Cenomanian source rock unit based on the available Rock Eval data to facilitate further discussion and perhaps stimulate future research initiatives.

4.3. Rock eval characteristics of the upper cenomanian source rock unit

The main characteristics of the upper Cenomanian organic-rich unit in the selected key wells are shown in Fig. 9. The overall trend indicates that most of the analyzed samples have poor potential indicated by low S2 values ($S2 < 2.5$ mg/g) and a highly variable TOC content (0.18–11.88 wt %; Fig. 9A). These samples have low HI values (40–150 mg HC/g TOC; Fig. 9B), and the few OI datapoints available show a widespread value distribution (1–198 CO₂/g TOC; Fig. 9C). Most of the samples are mature with T_{max} values ranging 430–450 °C (Fig. 9B) in proximity to the vitrinite reflectance trend line 0.88% (Fig. 9B). Collectively, most of the samples belonging to the upper Cenomanian organic-rich unit indicate a kerogen Type III composition and that gas would be the main expelled product (Fig. 9C).

Samples belonging to wells situated on the Halten Terrace and Sklinna Ridge indicate localized higher potential compared to the samples from the deeper Vøring Basin (Fig. 9). These samples exhibit increased TOC, S2 and HI values. In this regard, the samples which have a kerogen Type III–II composition in wells 6507/2–3 and 6506/11–3, is very intriguing (Fig. 9C).

Especially the samples from well 6506/11-3 stand out (Table 1 and Fig. 9), with TOC contents and S2 values averaging 2.53 wt % and 2.30 mg/g, respectively. However, these samples have low HI values, averaging 88 mg HC/g TOC, and the few OI datapoints available indicate an average of 48 mg CO₂/g TOC. No vitrinite reflectance data is available from well 6506/11–3. Still, based on the calculated average T_{max} value of 438 °C, the organic-rich unit is early mature. Collectively, this indicate that the upper Cenomanian organic-rich unit is oil-mature and kerogen Type III-dominated on the Sklinna Ridge.

Two samples from well 6507/2–3 indicate elevated potential for the upper Cenomanian – unit on the Halten Terrace (Fig. 9A and B), samples for the whole interval exhibit TOC contents and S2 values averaging 2.30 wt % and 4.11 mg/g, respectively. The HI is averaging 137 mg HC/g TOC, and there is no OI or vitrinite reflectance data available, but the organic-rich unit have an average T_{max} value of 432 °C, indicating that the organic matter is immature to early mature.

The general trend of the samples from the wells situated in the deeper Vøring Basin (i.e. 6607/5–1, 6705/10–1, 6603/5-1 S), suggest a poor potential indicated by low S2 values and TOC contents (Fig. 9A), as well as low HI values (Fig. 9B). Based on these parameters, the organic-rich unit appear to have a kerogen Type III composition (Fig. 9A and B). The average T_{max} values from samples in these wells (i.e. 432, 430, 407 °C) suggests that the upper Cenomanian organic-rich unit is immature on the eastern margins of the Gjallar Ridge and the Utgard High. The one sample from well 6705/10–1, which deviate from the general trend, exhibit high S2 values (5.82 mg/g), intermediate TOC contents (1.97 wt%) and good HI values (295 mg HC/g TOC). The same

sample also have low OI values (46 CO₂/g TOC) indicating higher qualities and a kerogen Type-II composition.

5. Discussion

The presence of an upper Cenomanian organic-rich unit with some source potential on the Halten Terrace and the Sklinna Ridge, as well as locally in the deeper parts of the Vøring Basin, is interesting because of its impact on the prospectivity of area. The apparent patchy and localized distribution and variable potential of the unit, suggests that its development was influenced by the fault-segmented internal configuration of the larger Vøring Basin and lateral variations in depositional environments with superimposed fluctuations in sedimentation rates, oxygen levels, organic productivity, and changing organic-matter preservation potential. Consequently, the most prolific zones are hard to predict. A discussion of the potential of the upper Cenomanian organic-rich unit and our proposed depositional model follows below.

5.1. Controls on source rock distribution and potential

The rift-related paleobathymetric configuration of the Vøring Basin exerted a first-order control on distribution and preservation of organic matter, directly influencing water mass circulation and bottom water oxygenation (e.g. Swiecicki et al., 1998; Fjellanger et al., 2005; Trabucho-Alexandre et al., 2012). The development and distribution of deep, silled basins, ridges and intrabasinal highs was controlled by the many faults and transfer zones which predominantly formed during the Late Jurassic – Early Cretaceous rifting event, and subsequent reactivation in the Late Cretaceous – Palaeocene (Færseth and Lien, 2002; Tsikalas et al., 2012; Zastrozhnov et al., 2020). This includes, amongst others, the Rås and Træna basins, who both experienced accelerated subsidence in the mid-Cenomanian – Turonian (Færseth and Lien, 2002; Lien, 2005; Zastrozhnov et al., 2018, 2020). Similar structural controls on water column circulation are well known from other basins and was crucial during deposition of the renowned Upper Jurassic source rock interval across the Norwegian Continental Shelf (e.g. Demaison et al., 1983; Miller, 1990; Cooper et al., 1995; Isaksen and Ledje, 2001; Marín et al., 2020).

Another critical factor for accumulating potential source rocks is sedimentation rate (e.g. Katz, 2005; Bohacs et al., 2005). Ideally, sedimentation rate should be below a critical threshold for organic matter to be preserved without experiencing a significant dilution effect (Ibach, 1982; Bohacs et al., 2005). Based on lithology, the mudstone dominated Cretaceous succession on the mid-Norwegian Continental shelf (Dalland et al., 1988; Gradstein et al., 2010) has a critical threshold around 21.13 m/m.y. (silty-clay lithology: Ibach, 1982). However, the relationship between sedimentation rate and organic content is complex (Tyson, 2001; Katz, 2005) as sedimentation rate varies across the basin (Færseth and Lien, 2002) due to variable distance and connection to the sediment source, position in relation to sea level, subsidence, climatic factors and sediment source rock composition (Prosser, 1993; Ravnås and Steel, 1998; Færseth and Lien, 2002). In addition to sedimentation rate, primary production and the following destruction of organic matter by biodegradation have a fundamental control on the amount of organic matter preserved cf. Tyson (2001) and Bohacs et al. (2005).

Structural highs which segmented the Vøring Basin during the Late Jurassic – Early Cretaceous rifting event, formed local sediment source areas which promoted high sedimentation rates (e.g. Bell et al., 2014). At a regional scale, rift-shoulder uplift of the conjugate continental landmasses bordering the North Atlantic Rift System (i.e. Western Norway and East Greenland) promoted fast filling of the deep basin bathymetry, presumably diluting the organic matter across the basin. However, the massive influx of continentally derived sediments (as evident by the thickness of the Cretaceous succession in the study area and adjacent basins), including residual material such as plant detritus, and increased fluvial run-off must periodically have enhanced primary

production (e.g. Wakeham and Lee, 1993).

The formation of a marine source rock unit is strongly dependent on nutrient influx to the basin either via fluvial sources or by coastal upwelling, both having the capability of promoting increased primary production of organic matter in the water column (Demaison et al., 1983; Calvert et al., 1996; Wesenlund et al., 2022). Enhanced primary production may also be caused by increased sea surface temperatures, rising sea level and flooding of coastal areas, as well as volcanic activity (Katz, 2005; Leckie et al., 2002; Scotese et al., 2021). The warm and humid climate, which prevailed during the Cretaceous greenhouse period, combined with a historically high eustatic sea-level and wide-spread volcanism related to the emplacement of large igneous provinces (LIPs) promoted increased biological productivity in the ocean (Leckie et al., 2002; Scotese et al., 2021). It may also be that increased chemical weathering and extensive deep weathering of exposed terranes in combination with increased precipitation rates and continental run-off contributed to the favorable conditions for maintaining high rates of primary production (Jenkyns, 1999, 2003; Leckie et al., 2002; Erba, 2004).

The Cenomanian - Turonian OAE 2 is represented by widespread deposition of organic-rich mudstones that imply expansion of anoxic and euxinic water layers on a global scale (Arthur et al., 1987; Leckie et al., 2002). This expansion is coupled to a transgressive development, leading to a global eustatic sea level highstand. The link between the major eustatic sea-level highstand at the Cenomanian - Turonian boundary (Haq et al., 1987; Miller et al., 2005) and deposition of organic-rich mudstones (Arthur et al., 1987, 1988) was established by Schlanger and Jenkyns (1976) and Jenkyns (1980). The increased eustatic sea-level was caused by major volcanism and corresponding active seafloor spreading, volume increase of mid-ocean ridges, thermal uplift of the seafloor, as well as the prevailing greenhouse climate which inhibited the establishment of polar icecaps (Schlanger et al., 1981; Arthur and Sageman, 2005; Pearce et al., 2009). The associated volcanic outgassing increased atmospheric CO₂ concentrations, terrestrial weathering, and nutrient flux (e.g. Sinton and Duncan, 1997; Adams et al., 2010). This development promoted eutrophication of the oceans and enhanced primary production (e.g. Turgeon and Creaser, 2008). The abundance of organic matter increased the consumption of dissolved oxygen by bacteria during decomposition. Eventually, this caused widespread anoxic conditions (i.e. OAE) and led to the deposition of organic-rich mudstones (Schlanger and Jenkyns, 1976; Schlanger et al., 1987; Arthur et al., 1987; Pearce et al., 2009).

The oxygen deficient conditions that characterize the early Aptian OAE1a is represented by an organic-rich unit on the Svalbard Platform (Midtkandal et al., 2016) and possibly also on the SW Barents Shelf (e.g. Hagset et al., 2022). This event was largely subject to the same controlling factors as OAE 2, and has been associated with volcanic outgassing from the Caribbean LIP and the High Arctic LIP (e.g. Maher, 2001; Maher et al., 2004; Corfu et al., 2013; Senger et al., 2014; Polteau et al., 2015; Midtkandal et al., 2016). The volcanism associated with HALIP, together with the Caribbean LIP (e.g. Serrano et al., 2011) is thus part of the larger picture explaining the occurrence of OAE 2 (e.g. Arthur et al., 1985; Adams et al., 2010; Zheng et al., 2013; Eldrett et al., 2014; Scaife et al., 2017).

5.2. Depositional model and source rock potential

It is well known that the fault-controlled topography/bathymetry in rift basins may restrict water circulation which leads to anoxic conditions that eventually favor source rock deposition (e.g. Heilbron et al., 2000). Following the extensive rifting phase in the Late Jurassic - Early Cretaceous, the mid-Norwegian margin developed to become a restricted marine or silled basin, which promoted anoxia and deposition of the renowned Upper Jurassic source rock. We suggest that the Early Cretaceous rift configuration on the mid-Norwegian margin resulted in similar conditions and thus periodically led to hypoxic to anoxic

conditions, particularly during the Early Cretaceous pulses of global anoxia (e.g. Beil et al., 2020), as recorded in exploration well 6608/2-1 S (OAE 1a in well 6608/2-1 S; see Zastrozhnov et al., 2020). It is very likely that the deep silled basin on the mid-Norwegian margin hosted a stratified water column controlled by the fault-related bathymetry and influx of fresh water. This physiography in combination with the recurrent global anoxic events promoted favorable conditions for preservation of organic matter (e.g. Demaison et al., 1983) and deposition of the Lower Cretaceous organic-rich units in the rift basins along the mid-Norwegian margin (Jongepier et al., 1996; Doré et al., 1997b) and on the Halten Terrace in particular (Fig. 5).

5.2.1. The upper cenomanian organic-rich unit on the Halten Terrace

The seismic investigation and evaluation of the upper Cenomanian organic-rich unit indicate that there is increased generation potential on the Sklinna Ridge and the northern part of Halten Terrace (i.e. wells 6506/11-3 and 6507/2-3; Table 1), with the organic-rich unit in well 6506/11-3 being recognized as the most prolific (Fig. 9). This unit has a kerogen Type III composition, which indicate significant terrestrial influence, possibly testifying to a proximal paleo-shoreline location for well 6506/11-3. The T_{max} values indicate an early mature source rock unit, whereas the dominant organo-facies, suggest potential for gas expulsion. We propose a depositional model for this unit which involves the development of an extended oxygen minimum zone in combination with significant contributions from terrestrial sources (Fig. 10). This model builds largely on the connection between deep-water circulation and productively as proposed by Arthur et al. (1987).

By Cenomanian times, a rifted seaway, being the precursor of the Norwegian Sea, had already been established for some time (Gradstein et al., 1999; Skogseid et al., 2000) and most likely experienced a steady inflow and exchange of water masses (Figs. 8B and 10). The onset of the OAE 2 greatly extended the oxygen minimum zone and left much of the water column in hypoxic to anoxic conditions (Fig. 10). These oxygen-deficient conditions might have been intensified or prolonged on the Sklinna High and Halten Terrace due to local upwelling (Fig. 10). Coastal upwelling typically forces deep, nutrient-rich water (e.g. nitrates and phosphates) to flow upwards through the water column promoting high biological productivity in the photic zone (Demaison and Moore, 1980; Demaison et al., 1983; Wesenlund et al., 2022, Fig. 10). Consequently, upwelling tends to intensify recycling of organic matter by oxygen-utilizing bacteria, which causes anoxic and hypoxic conditions in the mid to deeper water levels (Demaison and Moore, 1980; Demaison et al., 1983). This eventually promoted preservation of significant amounts of organic matter at the seafloor. Phosphate nodules, which commonly occur in sediments deposited under the influence of upwelling or other high productivity settings (e.g. Papadomanolaki et al., 2022; Wesenlund et al., 2022), have not been recorded in this study due to the lack of core data. However, in many reported cases, phosphate can only be detected as minor components in fossils and microfossils (e.g. Beil et al., 2020).

In the present case, nutrient-rich water was supplied from the deep oceanic realm of the Atlantic Ocean (Fig. 8B). The oceanic water was forced up against the margins of the Halten Terrace (i.e. against the KFC and YFZ) where oxygen minimum zones developed on the shallow marginal areas of the Halten Terrace and Sklinna Ridge due to increased primary production, potentially explaining why the upper Cenomanian organic-rich unit appear along the margins of these positive structural feature (i.e. Sklinna Ridge; Fig. 10). As the upper Cenomanian organic-rich unit only appears in a few wells (i.e. 6506/11-3 and 6507/2-3), it is possible that the anoxic conditions were restricted to specific areas along the margins of the Halten and Dønna Terraces (Fig. 10). Upwelling was most likely controlled by paleobathymetric conditions, water mass circulation, and prevailing winds in relation to the margin. These controlling factors could have restricted the extent and location of the oxygen minimum zone (Fig. 10). This, in combination with high sediment influx which diluted the organic-matter, ultimately hindered the

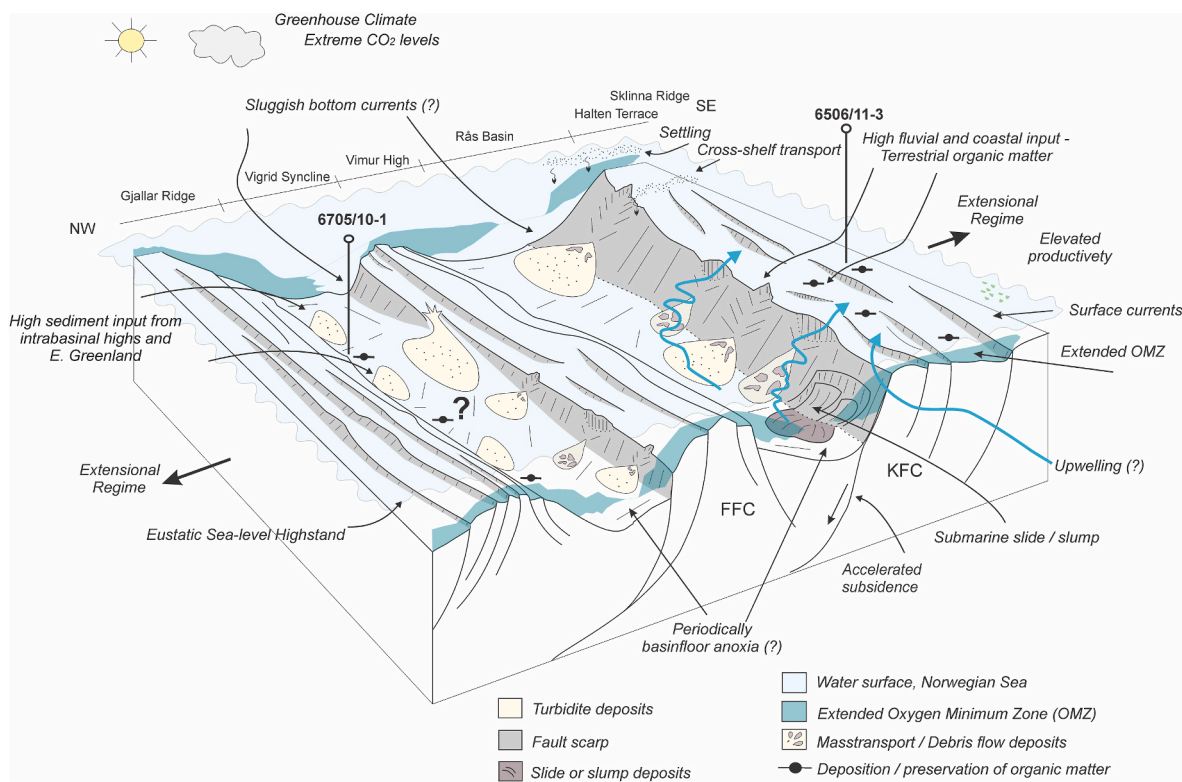


Fig. 10. Conceptual depositional model outlining the basin configuration and conditions during deposition of the upper Cenomanian organic-rich unit on the Sklinna Ridge, Rås Basin and Vigrid Syncline. The light red zone with dotted lines indicate an extended oxygen minimum zone connected to the OAE 2. Abbreviations: FFC: Fles Fault Complex, KFC: Klakk Fault Complex, OMZ: Oxygen minimum zone.

development of a thick, wide-spread prolific source rock at the Cenomanian to Turonian transition (Fig. 10).

The kerogen Type III organo-facies composition suggests that most of the organic matter was derived from terrestrial sources (Tissot et al., 1979; Tissot and Welte, 1984; Demaison et al., 1983). This may indicate that much of the organic matter entered the area via fluvial systems coming off the conjugate margins or via deposition from land-derived sediment gravity flows which promoted rapid burial (Fig. 10) (e.g. de Graciansky et al., 1987). Saller et al. (2006), for example document the presence of turbidites rich in leaves which act as a source rock in the Miocene Kutei Basin in Indonesia. These processes may to some extent explain the uneven vertical and spatial trend seen in the wireline values and TOC contents (well 6506/11-3; Fig. 5).

5.2.2. The upper cenomanian organic-rich unit in the Vøring Basin

The iuCn reflector has identical amplitude characteristics on the Sklinna Ridge, Golma Subbasin and in the Rås Basin. Despite similar characteristics, samples from well 6505/10-1 indicate that there is no source rock potential associated with the upper Cenomanian unit in the Golma Subbasin (Figs. 4 and 9). In the deeper Rås Basin and the Vigrid Syncline, the upper Cenomanian unit is confined between intrabasin highs, being delimited by the FFC and the KFC in the Rås Basin, and the FFC and the Gjallar Ridge in the Vigrid Syncline (Fig. 10). Samples from wells situated in the Vøring Basin (i.e. 6607/5-1, 6705/10-1, 6603/5-1 S) are immature – early mature for the upper Cenomanian organic-rich unit, possibly indicating increasing maturity towards the deeper basin segments. Samples from exploration well 6705/10-1 indicate an elevated petroleum potential with a mixture of kerogen Type II and III (Fig. 9). Collectively, this suggests that there is an increased possibility of a more prolific organic-rich unit locally in the deeper segments of the Vigrid Syncline (Fig. 10).

Sedimentation rates and oxygen levels appear to be the main controls on quantity and quality of organic matter for the upper Cenomanian

organic-rich unit (e.g. Arthur et al., 1985; Demaison and Moore, 1980; Demaison et al., 1983). Although hypoxic to anoxic water conditions may have been induced by elevated productivity during the OAE 2, the massive sedimented input hindered development of substantial quantities of organic matter (Fig. 10). Færseth and Lien (2002) reported the sedimentation rate to be on average 220 m/m.y. during the Cenomanian – Early Campanian period. Similar values were presented by Kjennerud and Vergara (2005) who indicated a sedimentation rate up to 300 m/m.y. This contrasts the critical threshold for dilution of organic-matter, reported to be 21.13 m/m.y. in silty-clay by Ibach (1982). The development of a high-quality prolific source rock unit therefore seems dependent on local or periodic reduction in sediment input (i.e. well 6705/10-1; Fig. 10), which further is controlled by paleobathymetric conditions and sediment fairways in the basin (Fig. 10).

Due to the well-developed oceanic conditions between Greenland and Norway in the Cretaceous (Gradstein et al., 1999), water mass circulation promoted oxygenated bottom water conditions (Fig. 10). However, during periods of fault-controlled restriction of the basin the bathymetry of the rotated fault blocks promoted reduced water mass circulation and oxygen-deficient bottom water conditions. In addition, biostratigraphic analysis indicate a periodically semi-restricted connection to the central Atlantic oceanic system (Gradstein et al., 1999). Typically, this configuration with a silled basin would create ideal conditions for the preservation of organic matter (Demaison and Moore, 1980; Demaison et al., 1983). However, massive sediment input due to a combination of rift-shoulder uplift of the conjugate margins and increased weathering rates and continental run-off driven by the Cretaceous climate, resulted in severe dilution of the organic matter (Fig. 10). Locally, in areas less affected by sediment dilution, accumulations of organic-rich deposits were preserved (i.e. wells 6603/5-1 S and 6705/10-1), possibly indicating a patchy distribution and moderate potential of the upper Cenomanian source rock unit in the deeper basin segments (Fig. 10). In addition, the Rås Basin has been identified as a

major Cretaceous depocenter during the middle Cenomanian to late Turonian times (Zastrozhnov et al., 2020), and concomitantly experienced accelerated subsidence and increased sedimentation during this period (Færseth and Lien, 2002; Zastrozhnov et al., 2020). High sedimentation rates may thus have impeded the possibility for sufficient and widespread accumulation of organic matter in this and other similar large depocenters on the mid-Norwegian margin (Bohacs et al., 2005).

In a regional perspective, the OAE 2 is represented by prolific organic-rich deposits relatively close to the study area, documented in the Sverdrup Basin, Galicia margin, Porcupine abyssal plain, and the North Sea (Doré et al., 1997b). On the mid-Norwegian margin, the occurrence of OAE 2 is evident by elevated TOC values and Rock-Eval parameters at the Cenomanian/Turonian boundary in several wells (Table 1). This confirms that OAE 2 stretched into the Norwegian – Greenland seaway and possible into the SW Barents Shelf (Fig. 8). However, the units are thin and condensed, making regional correlations problematic, but also indicate that the occurrence of OAE 2 is not enough for a prolific source rock unit to develop (e.g. Bohacs et al., 2005). The lack of a laterally extensive organic-rich unit on the mid-Norwegian margin, indicate that the extreme sedimentation rates and circulation of oxygenated waters were dominant factors. These factors promoted both severe dilution of the organic matter and biodegradation, which ultimately obstructed source rock development during OAE 2 on the mid-Norwegian margin. This contrasts the well-developed source rock units associated with the OAE 2 in the Sverdrup Basin and Arctic Canada (Leith et al., 1993; Lenniger et al., 2014; Herrle et al., 2015; Nøhr-Hansen et al., 2021). The conceptual model (Fig. 10) outlining the basin configuration, could thus be applicable in rift-basin setting where organic-rich units associated with OAEs are underdeveloped due to extreme sedimentation rates and circulation of oxygenated waters.

5.3. Implications for exploration

Although several of the Lower Cretaceous organic-rich units from the mid-Norwegian margin appear to coincide with global OAEs (e.g. Beil et al., 2020), our data demonstrate that most of these units are thin and strongly condensed or eroded on the terraces and local highs, and have been subject to deep burial. In addition, they accumulated during a period characterized by high sedimentation rates and consequently severe dilution of organic matter in the sediment depocenters. Although petroleum from Lower Cretaceous source rocks have been postulated from producing discoveries (Matapour and Karlsen, 2018), the occurrence of a regionally distributed and economically significant Lower Cretaceous source rock unit has not yet been confirmed. However, we cannot rule out the possibility that some of the Lower Cretaceous organic-rich units in the Vøring Basin once acted as potential sources, particularly in localized fault-bounded basins where the dilution effect and erosion had a limited impact on the preservation of organic matter.

The confirmation of a mature, regionally extensive upper Cenomanian source rock unit will have significant impact on the prospectivity of the deep, marginal basins bordering the North Atlantic Rift System (e.g. Bojesen-Koefoed et al., 2020). In the study area, however, our data shows that the unit has a limited thickness and modest quality (Table 1 and Fig. 9), indicating that it only holds a limited and very localized potential in proximity to intra-basinal highs and ridges. The sparsely drilled deep basins may of course contain thicker organic-rich accumulations holding greater source potential, particularly if the depocenters were subject to recurring anoxic conditions and avoided severe sediment dilution. Only continued exploration and drilling may reveal the presence of a prolific Upper Cretaceous source rock unit in the frontier basins on the mid-Norwegian margin.

6. Conclusions

By combining regional 2D reflection seismic data with wireline logs,

total organic carbon (TOC) contents, and Rock-Eval data, this study documents the presence of an upper Cenomanian organic-rich unit in the Vøring Basin. The unit exhibits TOC in the range of 0.18–11.88 wt %, S₂ in the range of 0.03–28.06 mg/g and Hydrogen content between 4 and 470 mg HC/g TOC. The unit shows the greatest potential in well 6506/11–3 and 6507/2–3 located on the Sklinna Ridge and Halten Terrace. Samples indicate that the organic-rich unit for the most part is characterized by a kerogen Type III–II composition and is in the immature – early mature stages, thus being capable of generating gas.

The corresponding reflector can be traced across the wider Vøring Basin and correlated to distal exploration wells. The upper Cenomanian organic-rich unit is encountered in well 6705/10–1 on the NW flank of the Vigrid Syncline, where the organic-rich unit exhibit a kerogen Type II composition, possibly indicating periods of basin floor anoxic conditions and locally reduced sedimentation rates.

We suggest that the rifted paleo-basin configuration of the Vøring basin in combination with the global anoxic event at the transition between the Cenomanian - Turonian may have resulted in local accumulations of organic material. The configuration of the margin and the shallow character of the Halten Terrace promoted preservation of organic matter attributed to the development of an extended oxygen minimum zone during OAE 2 and local upwelling of deep oceanic water masses from the Atlantic realm. Moreover, the combination of a eustatic sea-level highstand and high input of terrestrial sediments and organic matter, promoted deposition of the upper Cenomanian organic-rich unit. Several other thin and condensed Lower Cretaceous organic-rich units are present on the Halten Terrace. Although these units commonly exhibit elevated TOC contents, they only hold limited potential due to their meagre thickness, localized distribution, and because they were presumably deposited during a time of severe organic matter dilution due to massive sediment flux into the basin.

The well-developed oceanic conditions between Greenland and Norway were parts of the northern Atlantic Ocean where widespread deposition of organic-rich mudstones associated with the OAE 2 occurred. The rift basin configuration with paleobathymetric barriers partly hindered water mass circulation. In combination with OAE 2, this led to hypoxic to anoxic conditions. Thus, establishing favorable circumstances for preservation of organic matter. The close proximity to the conjugate margins ensured high sedimentation rates, diluting much of the organic-matter. However, areas shielded from the highest sedimentation rates, erosion, and gravity flows, could have facilitated conditions suitable for organic-matter preservation. Such areas occur on the Halten Terrace and in the Vigrid Syncline. Hopefully, this could renew interest and research on global anoxic events on the Norwegian Continental Shelf. Once we have a clear understanding about the dynamic and complex distribution of organic-rich sediments, risk involved in exploration could be significantly reduced.

Declaration of competing interest

The authors declare that they have no known competing financial interests or personal relationships that could have appeared to influence the work reported in this paper.

Data availability

Data will be made available on request.

Acknowledgements

The first author is grateful to Wintershall-Dea for funding this research through a three-year PhD position at UiT - The Arctic University of Norway. The authors are grateful to TGS for allowing to publish their multient data. Fredrik Wesenlund is thanked for his guidance in Python and for providing the code to the source rock evaluation plots. The Associate Editor and the anonymous reviewers are gratefully

acknowledged for their comments and suggestions which improved the manuscript.

Appendix A. Supplementary data

Supplementary data to this article can be found online at <https://doi.org/10.1016/j.marpetgeo.2023.106102>.

References

- Abdelmalak, M.M., Planke, S., Faleide, J.I., Jerram, D.A., Zastrozhnov, D., Eide, S., Myklebust, R., 2016. The development of volcanic sequences at rifted margins: new insights from the structure and morphology of the Voring Escarpment, mid-Norwegian Margin. *J. Geophys. Res. Solid Earth* 121, 5212–5236. <https://doi.org/10.1002/2015JB012788>.
- Adams, D.D., Hurtgen, M.T., Sageman, B.B., 2010. Volcanic triggering of a biogeochemical cascade during oceanic anoxic event 2. *Nat. Geosci.* 3, 201–204.
- Arthur, M.A., Sageman, B.B., 1994. Marine black shales - depositional mechanisms and environments of ancient deposits. *Annu. Rev. Earth Planet Sci.* 22, 499–551.
- Arthur, M.A., Sageman, B.B., 2005. sea-level control on source-rock development: perspectives from the holocene black sea, the mid-cretaceous western interior basin of north America, and the late devonian appalachian basin. In: Harris, N.B. (Ed.), *The Deposition of Organic Carbon-Rich Sediments: Models, Mechanisms and Consequences*. SEPM Special Publication 82. SEPM, Tulsa, Oklahoma, pp. 35–59.
- Arthur, M.A., Schlanger, S.O., 1979. Cretaceous "oceanic anoxic events" as causal factors in development of reef-reservoired giant oil fields. *AAPG (Am. Assoc. Pet. Geol.) Bull.* 63, 870–885.
- Arthur, M.A., Dean, W.E., Schlanger, S.O., 1985. Variations in the global carbon cycle during the cretaceous related to climate, volcanism, and changes in atmospheric CO₂. In: Sundquist, E., Broecker, W. (Eds.), *The Carbon Cycle and Atmospheric CO₂: Natural Variations Archaean to Present*. Geophysical Monograph Series. 32. American Geophysical Union, Washington D.C., pp. 504–529.
- Arthur, M.A., Schlanger, S.O., Jenkens, H.C., 1987. The Cenomanian-Turonian Oceanic Anoxic Event, II. Palaeoceanographic controls on organic-matter production and preservation. In: Brooks, J., Fleet, A.J. (Eds.), *Marine Petroleum Source Rocks*. Geological Society, London, Special Publications. 26. Blackwell Scientific Publications, London, pp. 401–420.
- Arthur, M.A., Dean, W.E., Pratt, L.M., 1988. Geochemical and climatic effects of increased marine organic carbon burial at the Cenomanian/Turonian boundary. *Nature* 335 (6192), 714–717. <https://doi.org/10.1038/335714a0>.
- Arthur, M.A., Jenkens, H.C., Brumsack, H.-J., Schlanger, S.O., 1990. Stratigraphy, geochemistry, and paleoceanography of organic carbon-rich Cretaceous sequences. In: Ginsburg, R.N., Beaudoin, B. (Eds.), *Cretaceous Resources, Events Rhythms: Background and Plans for Research*. NATO ASI Series 304. Kluwer Academic Publishers, Dordrecht, pp. 75–119.
- Beil, S., Kuhnt, W., Holbourn, A., Scholz, F., Oxmann, J., Wallmann, K., Lorenzen, J., Aquit, M., Chellai, E.H., 2020. Cretaceous Oceanic Anoxic events prolonged by phosphorus cycle feedbacks. *Clim. Past* 16, 757–782.
- Bell, R.E., Jackson, C.A.-L., Elliott, G.M., Gawthorpe, R.L., Sharp, I.R., Michelsen, L., 2014. Insights into the development of major rift-related unconformities from geologically constrained subsidence modelling: Halten Terrace, offshore mid Norway. *Basin Res.* 26, 203–224.
- Blystad, P., Færseth, R.B., Larsen, B.T., Skogseid, J., Tørdabakken, B., 1995. Structural elements of the Norwegian continental shelf. Part II: the Norwegian Sea Region. *Norwegian Petroleum Directorate Bulletin* 8, 45p.
- Bohacs, K.M., Jr., G.J.G., Carroll, A.R., Mankiewicz, P.J., Miskell-Gerhardt, K.J., Schwalbach, J.R., Wegner, M.B., Simo, J.A.T., 2005. Production, destruction and dilution—the many paths to source-rock development. *Soc. Sediment. Geol.* 82, 61–101.
- Bojesen-Koefoed, J.A., Alsen, P., Bjerager, M., Hovikoski, J., Ineson, J., Nytoft, H.P., Nøhr-Hansen, H., Petersen, H.I., Pilgaard, A., Vosgerau, H., 2020. A mid-Cretaceous petroleum source-rock in the North Atlantic region? Implications of the Nanok-1 fully cored borehole, Hold with Hope, northeast Greenland. *Mar. Petrol. Geol.* 117, 104414 <https://doi.org/10.1016/j.marpetgeo.2020.104414>.
- Bralower, T.J., Sliter, W.V., Arthur, M.A., Leckie, R.M., Allard, D., Schlanger, S.O., 1993. Dysoxic/anoxic episodes in the aptian-albian (early cretaceous). In: Pringle, M., Sager, W.W., Sliter, W.V., Stein, S. (Eds.), *The Mesozoic Pacific: Geology, Tectonics, and Volcanism*, vol. 77. American Geophysical Union Monograph, pp. 5–37.
- Brekke, H., 2000. The tectonic evolution of the Norwegian sea continental margin with emphasis on the Vøring and More basins. Geological Society, London, Special Publications 167 (1), 327–378. <https://doi.org/10.1144/gsl.sp.2000.167.01.13>.
- Brekke, H., Dahlgren, S., Nyland, B., Magnus, C., 1999. The prospectivity of the Vøring and Møre basins on the Norwegian continental margin. In: Fleet, A.J., Boldy, S.A.R. (Eds.), *Petroleum Geology of Northwest Europe: Proceedings of the 5th Conference*. Geological Society of London, pp. 231–246.
- Brekke, H., Sjulstad, H.I., Magnus, C., Williams, R.W., 2001. Sedimentary environments offshore Norway -An overview. In: Martinsen, O.J., Dreyer, T. (Eds.), *Sedimentary Environments Offshore Norway -Palaeozoic to Recent*. NPF Special Publication, pp. 7–37.
- Calvert, S.E., Bustin, R.M., Ingall, E.D., 1996. Influence of water column anoxia and sediment supply on the burial and preservation of organic carbon in marine shales. *Geochem. Cosmochim. Acta* 60, 1577–1593.
- Cohen, K.M., Finney, S.C., Gibbard, P.L., Fan, J.-X., 2013. The ICS international chronostratigraphic chart. *Episodes* 36 (3), 199–204.
- Cooper, B.S., Barnard, P.C., Telnaes, N., 1995. The kimberidge clay formation of the North sea. In: Katz, B.J. (Ed.), *Petroleum Source Rocks*. Casebooks in Earth Sciences. Springer, Berlin, Heidelberg. https://doi.org/10.1007/978-3-642-78911-3_6.
- Corfu, F., Polteau, S., Planke, S., Faleide, J.I., Svensen, H., Zayoncheck, A., Stolbov, N., 2013. U-Pb geochronology of cretaceous magmatism on svalbard and Franz Josef land, Barents sea large igneous province. *Geol. Mag.* 150, 1127–1135.
- Dalland, A., Worsley, D., Ofstad, K., 1988. A lithostratigraphic scheme for the Mesozoic and Cenozoic succession offshore mid- and northern Norway. *NPD Bulletin* 4, 63.
- Demaison, G.J., Moore, G.T., 1980. Anoxic environments and oil source bed genesis. *AAPG (Am. Assoc. Pet. Geol.) Bull.* 64, 1179–1209.
- Demaison, G.J., Hoick, A.J.J., Jones, R.W., Moore, G.T., 1983. Predictive source bed stratigraphy: a guide to regional petroleum occurrence. In: *Proceedings of the 11th World Petroleum Congress*, vol. 2. John Wiley & Sons, Ltd., London, p. 17.
- Doré, A.G., Lundin, E.R., Flichler, C., Olesen, O., 1997a. Patterns of basement structure and reactivation along the NE Atlantic margin. *J. Geol. Soc.* 154, 85–92.
- Doré, A.G., Lundin, E.R., Birkeland, Ø., Eliassen, P.E., Jensen, L.N., 1997b. The NE Atlantic Margin: implications of late Mesozoic and Cenozoic events for hydrocarbon prospectivity. *Petrol. Geosci.* 3, 117–131.
- Doré, A.G., Lundin, E.R., Jensen, L.N., Birkeland, Ø., Eliassen, P.E., Fichler, C., 1999. Principal tectonic events in the evolution of the northwest European Atlantic margin, 1. In: Geological Society, London, *Petroleum Geology Conference Series*, vol. 5. Geological Society of London, pp. 41–61.
- Eldrett, J.S., Minisini, D., Bergman, S.C., 2014. Decoupling of the carbon cycle during ocean anoxic event 2. *Geology* 42 (7), 567–570.
- Erba, E., 2004. Calcareous nannofossils and Mesozoic oceanic anoxic events. *Mar. Micropaleontol.* 52, 85–106. <https://doi.org/10.1016/j.marmicro.2004.04.007>.
- Erbacher, J., Thurow, J., Littke, R., 1996. Evolution patterns of radiolaria and organic matter variations: a new approach to identify sea-level changes in mid-cretaceous pelagic environments. *Geology* 24 (6), 499–502.
- Espitalié, J., Madec, M., Tissot, B., Mennig, J.J., Leplat, P., 1977. Source rock characterization method for petroleum exploration. Paper OTC (Offshore Technology Conference) 2935, 439–444.
- Factpages, N.P.D., 2022 [WWW Document] Norwegian Petroleum Directorate, Factpages for exploration wells. <https://factpages.npd.no/en/wellbore>. (Accessed 15 September 2022). Accessed.
- Faleide, J.I., Tsikalas, F., Breivik, A.J., Mjelde, R., Ritzmann, O., Engen, O., Wilson, J., Eldholm, O., 2008. Structure and evolution of the continental margin off Norway and Barents Sea. *Episodes* 31, 82–91.
- Faleide, J.I., Bjørlykke, K., Gabrielsen, R.H., 2015. *Geology of the Norwegian Continental Shelf*. Chapter 25 from the Book. In: second ed. "Bjørlykke, K Petrol. Geosci.: from Sedimentary Environments to Rock Physics", pp. 603–637.
- Færseth, R.B., Lien, T., 2002. Cretaceous evolution in the Norwegian Sea – a period characterized by tectonic quiescence. *Mar. Petrol. Geol.* 19, 1005–1027. [https://doi.org/10.1016/S0264-8172\(02\)00112-5](https://doi.org/10.1016/S0264-8172(02)00112-5).
- Fjellanger, E., Surlyk, F., Wamsteeker, L.C., Midtun, T., 2005. Upper Cretaceous basinfloor fans in the Vøring Basin, mid Norway shelf. In: Wandas, B.T.G., Nystuen, J.P., Eide, E., Gradstein, F. (Eds.), *Onshore-offshore Relationships on the North Atlantic Margin*. Proceedings of the Norwegian Petroleum Society Conference, October 2002, Trondheim, Norway. Trondheim.
- Garner, L.H., Farrimond, P., Nuzzo, M., 2017. Alternative Source Rocks on the Norwegian Continental Shelf: Potential Cretaceous Sourcing in Deepwater Basins. AAPG/SEG International Conference & Exhibition, London, England. Oct 15 – 18, 2017.
- Gernign, L., Ringenbach, J.-C., Planke, S., Jonquet-Kolsto, H., 2003. Extension, crustal structure and magmatism at the outer Vøring Basin, Norwegian margin. *J. Geol. Soc.* 160, 197–208. <https://doi.org/10.1144/0016-764902-055> (London).
- Gernign, L., Zastrozhnov, D., Planke, S., Abdelmalak, M.M., Maharjan, D., Manton, B., Faleide, J.I., Myklebust, R., 2021. A digital compilation of structural and magmatic elements of the Mid-Norwegian continental margin (version 1.0). *Norw. J. Geol.*
- Graciansky, P.C. de, Brosse, E., Deroo, G., Herbin, J.-P., Müller, C., Sigal, J., Schaaf, A., Montadert, L., 1987. Organic-rich sediments and palaeoenvironmental reconstructions of the cretaceous north Atlantic. In: Brooks, J., Fleet, A.J. (Eds.), *Marine Petroleum Source Rocks*. Geological Society Special Publication No. 26, pp. 317–344.
- Gradstein, F.M., Kaminski, M.A., Agterberg, F.P., 1999. Biostratigraphy and paleoceanography of the Cretaceous seaway between Norway and Greenland. *Earth Sci. Rev.* 46, 27e98. [https://doi.org/10.1016/S0012-8252\(99\)00018-5](https://doi.org/10.1016/S0012-8252(99)00018-5).
- Gradstein, F.M., Anthonissen, E., Brunstad, H., Charnock, M., Hammer, Ø., Hellem, T., Lervik, K.S., 2010. Norwegian offshore stratigraphic lexicon (NORLEX). *Newsl. Stratigr.* 44, 73–86.
- Hagset, A., Grundvåg, S.A., Badics, B., Davies, R., Rotevatn, A., 2022. Tracing lower cretaceous organic-rich units across the SW Barents shelf. *Mar. Petrol. Geol.* 140, 105664.
- Hansen, L.A.S., Hodgson, D.M., Pontén, A., Thrana, C., Obradors Latre, A., 2021. Mixed axial and transverse deep-water systems: the cretaceous post-rift lysing formation, offshore Norway. *Basin Res.* 33, 2229–2251. <https://doi.org/10.1111/bre.12555>.
- Haq, B.U., Hardenbol, J., Vail, P.R., 1987. Chronology of fluctuating sea levels since the Triassic (250 million years ago to present). *Science* 235, 1156–1166.
- Heilbron, M., Mohriak, W.U., Valeriano, C.M., Milani, E.J., Almeida, J., Tupinamba', M., 2000. From collision to extension, the roots of the southeastern continental margin of Brazil. In: Mohriak, W.U., Talwani, M. (Eds.), *Atlantic Rifts and Continental Margins*, vol. 115. AGU Geophysical Monograph, pp. 1–32.

- Herrle, J.O., Schröder-Adams, C.J., Davis, W., Pugh, A.T., Galloway, J.M., Fath, J., 2015. Mid-Cretaceous high arctic stratigraphy, climate, and oceanic anoxic events. *Geology* 43 (5), 403–406.
- Ibach, L.E.J., 1982. Relationship between sedimentation-rate and total organic-carbon content in ancient marine-sediments. *AAPG (Am. Assoc. Pet. Geol.) Bull.* 66, 170–188.
- Isaksen, G.H., Ledje, K.H.I., 2001. Source rock quality and hydrocarbon migration pathways within the greater utsira high area, viking graben, Norwegian North Sea. *AAPG (Am. Assoc. Pet. Geol.) Bull.* 85, 861–883.
- Isaksen, D., Tonstad, K., 1989. A Revised Cretaceous and Tertiary Lithostratigraphic Nomenclature for the Norwegian North Sea. *NPD-Bulletin*. No 5. <http://www.npd.no/en/Publications/NPDbulletins/255-Bulletin-5/>.
- Jenkyns, H.C., 1980. Cretaceous anoxic events - from continents to oceans. *J. Geol. Soc.* 137, 171–188.
- Jenkyns, H.C., 1999. Mesozoic anoxic events and palaeoclimate. *Zbl. Geol. Paläontol.* 943–949, 1997.
- Jenkyns, H.C., 2003. Evidence for rapid climate change in the Mesozoic-Palaeogene greenhouse world. *Philosophical Transactions of the Royal Society A* 361, 1885. <https://doi.org/10.1098/rsta.2003.1240>. –1916.
- Jongepier, K., Rui, J.C., Grue, K., 1996. Triassic to Early Cretaceous stratigraphic and structural development of the northeastern Møre Basin margin, off Mid-Norway. *Nor. Geol. Tidsskr.* 76, 199–214.
- Katz, B., 2005. Controlling factors on source rock development—a review of productivity, preservation, and sedimentation rate. *Soci. Sed. Geol.* 82, 7–16.
- Kjennerud, T., Vergara, L., 2005. Cretaceous to palaeogene 3D palaeobathymetry and sedimentation in the Vøring basin, Norwegian sea. *Geol. Soc. Lond. Petrol. Geol. Conf. ser.* 6, 815.
- Klemme, H.D., Ulmishek, G.F., 1991. Effective petroleum source rocks of the World: stratigraphic distribution and controlling depositional factors. *AAPG Bull.* 75, 1809–1851.
- Leckie, R.M., Bralower, T.J., Cashman, R., 2002. Oceanic anoxic events and plankton evolution: biotic response to tectonic forcing during the mid-Cretaceous. *Paleoceanography* 17, 13–29.
- Leith, T.L., Weiss, H.M., Mørk, A., Århus, N., Elvebakk, G., Embry, A.F., Brooks, P.W., Stewart, K.R., Pchelina, T.M., Bro, E.G., Verba, M.L., Danyushevskaya, A., Borisov, A.V., 1993. Mesozoic hydrocarbon source rocks of the Arctic region. In: Vorren, T.O., Bergsager, E., Dahl-Stammes, A., Holter, E., Johansen, Å., Lie, Å., Lund, T.B. (Eds.), *Arctic Geology and Petroleum Potential*. Elsevier, Amsterdam, pp. 1–25.
- Lenniger, M., Nøhr-Hansen, H., Hills, L.V., Bjerrum, C.J., 2014. Arctic black shale formation during cretaceous oceanic Anoxic Event 2. *Geology* 42, 799–802.
- Lien, T., 2005. From rifting to drifting: effects on the development of deep-water hydrocarbon reservoirs in a passive margin setting. *Norwegian Sea. Nor. J. Geol./Nor. Geol. Foren.* 85 (4).
- Løseth, H., Wensaas, L., Gading, M., Duffaut, K., Springer, M., 2011. Can hydrocarbon source rocks be identified on seismic data? *Geology* 39, 1167–1170.
- Lundin, E.R., Doré, A.G., Ronning, K., Kyrkjøbo, R., 2013. Repeated inversion and collapse in the late cretaceous-zenozoic northern voring basin, offshore Norway. *Petrol. Geosci.* 19, 329–341. <https://doi.org/10.1144/petgeo2012-022>.
- Maher, H.D., 2001. Manifestations of the Cretaceous high arctic large igneous province in Svalbard. *J. Geol.* 109, 91–104.
- Maher, H.D., Hays, T., Shuster, R., Mutrux, J., 2004. Petrography of the lower cretaceous sandstones of spitsbergen. *Polar Res.* 23, 147–165.
- Mann, U., Zweigel, J., Øygaard, K., Gjeldvik, G., 2002. Source rock prediction in deepwater frontier exploration areas: an integrated study of the Cretaceous in the Vøring Basin. In: Research, S.P. (Ed.), *AAPG Hedberg Conference: Hydrocarbon Habitat of Volcanic Rifted Passive Margins, Stavanger, Norway*.
- Marín, D., Hellenen, S., Escalona, A., Olausen, S., Cedeno, A., Nøhr-Hansen, H., Ohm, S., 2020. The Middle Jurassic to lowermost Cretaceous in the SW Barents Sea: interplay between tectonics, coarse-grained sediment supply and organic matter preservation. *Basin Res.* 33 (2), 1033–1055. <https://doi.org/10.1111/bre.12504>.
- Martinsen, O.J., Lien, T., Jackson, C., 2005. Cretaceous and Paleogene turbidite systems in the North Sea and Norwegian Sea Basins: source, staging area and basin physiography controls on reservoir development. In: Doré, A.G., Vining, B.A. (Eds.), *Petroleum Geology: Northwest Europe and Global Perspectives- Proceedings of the 6th Petroleum Geology Conference*, pp. 1147–1164.
- Matapour, Z., Karlsen, D.A., 2018. Ages of Norwegian oils and bitumen based on agespecific biomarkers. *Petrol. Geosci.* 24, 92–101. <https://doi.org/10.1144/petgeo2016-119>.
- Midtkandal, I., Svensen, H.H., Planke, S., Corfu, F., Polteau, S., Torsvik, T.H., Faleide, J. I., Grundvåg, S.A., Selnes, H., Kurschner, W., Olausen, S., 2016. The aptian (early cretaceous) oceanic anoxic event (OAE1a) in svalbard, Barents Sea, and the absolute age of the barremian-aptian boundary. *Palaeogeogr. Palaeoclimatol.* 463, 126–135.
- Miller, R.G., 1990. A paleoceanographic approach to the kimmeridge clay formation. In: Huc, A.Y. (Ed.), *Deposition of Organic Facies*, American Association of Petroleum Geologists, Studies in Geology 30, 13–26. <https://doi.org/10.1306/St30517C2>.
- Miller, K.G., Komazin, M.A., Browning, J.V., Wright, J.D., Mountain, G.S., Katz, M.E., Sugarman, P.J., Cramer, B.S., Christie-Blick, N., Pekar, S.F., 2005. The Phanerozoic record of global sea-level change. *Science* 310, 1293–1298. <https://doi.org/10.1126/science.1116412>.
- Nøhr-Hansen, H., Pedersen, G.K., Knutz, P.K., Bojesen-Koefoed, J.A., Sliwinska, K.K., Hovikoski, J., Ineson, J.R., Kristensen, L., Therkelsen, J., 2021. The Cretaceous succession of northeast Baffin Bay: stratigraphy, sedimentology and petroleum potential. *Mar. Petrol. Geol.* 133 <https://doi.org/10.1016/j.marpetgeo.2021.105108>.
- Papadomanolaki, N.M., Lenstra, W.K., Wolthers, M., Slomp, C.P., 2022. Enhanced phosphorus recycling during past oceanic anoxia amplified by low rates of apatite authigenesis. *Sci. Adv.* 8 (26) <https://doi.org/10.1126/sciadv.abn2370>.
- Pearce, M.A., Jarvis, I., Tocher, B.A., 2009. The Cenomanian-Turonian boundary event, OAE2 and palaeoenvironmental change in epicontinental seas: new insights from the dinocyst and geochemical records. *Palaeogeogr. Palaeoclimatol. Palaeoecol.* 280, 207–234. <https://doi.org/10.1016/j.pa-laeco.2009.06.012>.
- Pedersen, T.F., Calvert, S.E., 1990. Anoxia vs productivity - what controls the formation of organic-carbon-rich sediments and sedimentary-rocks. *AAPG (Am. Assoc. Pet. Geol.) Bull.* 74, 454–466.
- Peron-Pinvidic, G., Osmundsen, P.T., 2018. The Mid Norwegian-NE Greenland conjugate margins: rifting evolution, margin segmentation, and breakup. *Mar. Petrol. Geol.* 98, 162–184.
- Peters, K.E., 1986. Guidelines for evaluating petroleum source rock using programmed pyrolysis. *AAPG (Am. Assoc. Pet. Geol.) Bull.* 70, 318–329.
- Peters, K.E., Cassa, M.R., 1994. Applied source rock geochemistry. In: Magoon, L.B., Dow, W.G. (Eds.), *The Petroleum System - from Source to Trap*. AAPG, pp. 93–120.
- Planke, S., Rasmussen, T., Rey, S., Myklebust, R., 2005. Seismic characteristics and distribution of volcanic intrusions and hydrothermal vent complexes in the Vøring and Møre basins. In: Geological Society, London, Petroleum Geology Conference Series. Geological Society of London, pp. 833–844.
- Polteau, S., Hendriks, B.W.H., Planke, S., Ganerød, M., Corfu, F., Faleide, J.I., Midtkandal, I., Svensen, H.S., Myklebust, R., 2015. The early cretaceous Barents sea sill complex: distribution, 40Ar/39Ar geochronology, and implications for carbon gas formation. *Palaeogeogr. Palaeoclimatol. Palaeoecol.* <https://doi.org/10.1016/j.palaeo.2015.07.007>.
- Prosser, S., 1993. Rift-related Linked Depositional Systems and Their Seismic Expression, vol. 71. Geological Society, London, Special Publications, pp. 35–66.
- Ravnås, R., Steel, R.J., 1998. Architecture of marine rift-basin successions. *AAPG (Am. Assoc. Pet. Geol.) Bull.* 82, 110–146.
- Rotevatn, A., Kristensen, T.B., Ksienzyk, A.K., Wemmer, K., Henstra, G.A., Midtkandal, I., Grundvåg, S.-A., Andresen, A., 2018. Structural inheritance and rapid rift-length establishment in a multiphase rift: the East Greenland rift system and its Caledonian orogenic ancestry. *Tectonics* 37, 1858–1875. <https://doi.org/10.1029/2018TC005018>.
- Saller, A., Lin, R., Dunham, J., 2006. Leaves in turbidite sands: the main source of oil and gas in the deep-water Kutei Basin, Indonesia. *AAPG (Am. Assoc. Pet. Geol.) Bull.* 90, 1585–1608.
- Scaife, J.D., Ruhl, M., Dickson, A.J., Mather, T.A., Jenkyns, H.C., Percival, L.M.E., Heselbo, S.P., Cartwright, J., Eldrett, J.S., Bergman, S.C., Minisini, D., 2017. Sedimentary mercury enrichments as a marker for submarine large igneous province volcanism? Evidence from the mid-cenomanian event and oceanic anoxic event 2 (late cretaceous). *G-cubed* 18, 4253–4275.
- Schlanger, S.O., Jenkyns, H.C., 1976. Cretaceous oceanic anoxic events: causes and consequences. *Geol. Mijnbouw* 55, 179–184.
- Schlanger, S.O., Jenkyns, H.C., Premoli-Silva, I., 1981. Volcanism and vertical tectonics in the Pacific Basin related to global Cretaceous transgressions. *Earth Planet Sci. Lett.* 52, 435–449.
- Schlanger, S.O., Arthur, M.A., Jenkyns, H.C., Scholle, P.A., 1987. The Cenomanian-Turonian Oceanic Anoxic Event, I. Stratigraphy and distribution of organic carbon-rich beds and the marine 613C excursion. *Geol. Soc. Lond. Spec. Publ.* 26 (1), 371–399. <https://doi.org/10.1144/GSL.SP.1987.026.01.24>.
- Schröder-Adam, C.J., Herrle, J.O., Selby, D., Quessel, A., Froude, G., 2019. Influence of the high arctic igneous province on the cenomanian/turonian boundary interval, Sverdrup Basin, high Canadian arctic. *Earth Planet Sci. Lett.* 511, 76–88.
- Scotese, C.R., Song, H., Mills, B.J.W., van der Meer, D.G., 2021. Phanerozoic paleotemperatures: the earth's changing climate during the last 540 million years. *Earth Sci. Rev.* 215, 103–503.
- Senger, K., Tveranger, J., Ogata, K., Braathen, A., Planke, S., 2014. Late mesozoic magmatism in svalbard: a review. *Earth Sci. Rev.* 139, 123–144.
- Serrano, L., Ferrari, L., Martínez, M.L., Petrone, C.M., Jaramillo, C., 2011. An integrative geologic, geochronologic and geochemical study of Gorgona Island, Colombia: implications for the formation of the Caribbean Large Igneous Province. *Earth Planet Sci. Lett.* 309 (3–4), 324–336.
- Sheriff, R.E., 2002. *Cyclopedic Dictionary of Applied Geophysics*, fourth ed. Society of Exploration Geophysicists, Tulsa, Okla.
- Sinton, C.W., Duncan, R.A., 1997. Potential links between ocean plateau volcanism and global ocean anoxia at the Cenomanian-Turonian boundary. *Econ. Geol.* 92 (7–8), 836–842.
- Skogseid, J., Planke, S., Faleide, J.I., Pedersen, T., Eldholm, O., Neverdal, F., 2000. NE Atlantic continental rifting and volcanic margin formation. In: Nøttvedt, A. (Ed.), *Dynamics of the Norwegian Margin*. Geological Society Special Publications, pp. 295–326.
- Swiecicki, T., Gibbs, P.B., Farrow, G.E., Coward, M.P., 1998. A tectonostratigraphic framework for the mid-Norway region. *Mar. Petrol. Geol.* 15, 245–276.
- Tissot, B.P., Welte, D.H., 1984. From kerogen to petroleum. In: *Petroleum Formation and Occurrence*. Springer, Berlin Heidelberg, pp. 160–198.
- Tissot, B., Deroo, G., Herbin, J.P., 1979. Organic matter in Cretaceous sediments of the North Atlantic: contribution to sedimentology and paleogeography. In: Talwani, M., Hay, W.W., Ryan, W.B.F. (Eds.), *Deep Drilling Results in the Atlantic Ocean: Continental Margins and Paleoenvironment*, Maurice Ewing Ser., vol. 3. Am. Geophys. Union, Washington, pp. 362–374.
- Trabucho-Alexandre, J., Hay, W.W., De Boer, P.L., 2012. Phanerozoic environments of black shale deposition and the Wilson Cycle. *Solid Earth* 3, 29–42. <https://doi.org/10.5194/se-3-29-2012>.

- Tsikalas, F., Faleide, J.I., Eldholm, O., Wilson, J., 2005. Late Mesozoic-Cenozoic structural and stratigraphic correlations between the Conjugate mid-Norway and NE Greenland continental margins. In: Doré, A.G., Vining, B.A. (Eds.), *Petroleum Geology: North-West Europe and Global Perspectives—Proceedings of the 6th Petroleum Geology Conference*, pp. 785–801.
- Tsikalas, F., Faleide, J.I., Eldholm, O., Blaich, O.A., 2012. The NE Atlantic conjugate margins. In: Roberts, D.G., Bally, A.W. (Eds.), *Phanerozoic Passive Margins, Cratonic Basins and Global Tectonic Maps*, pp. 141–201.
- Tsikalas, F., Faleide, J.I., Kalač, A., 2019. New insights into the Cretaceous-Cenozoic tectono-stratigraphic evolution of the southern Lofoten margin, offshore Norway. *Mar. Petrol. Geol.* 110, 832–855. <https://doi.org/10.1016/j.marpetgeo.2019.07.025>.
- Turgeon, S.C., Creaser, R.A., 2008. Cretaceous oceanic anoxic event 2 triggered by a massive magmatic episode. *Nature* 454, 323–327. <https://doi.org/10.1038/nature07076>.
- Tyson, R.V., 2001. Sedimentation rate, dilution, preservation and total organic carbon: some results of a modelling study. *Org. Geochem.* 32 (2), 333–339.
- Vergara, L., Wreglesworth, I., Trayfoot, M., Richardsen, G., 2001. The distribution of Cretaceous and Paleocene deep-water reservoirs in the Norwegian Sea basins. *Petrol. Geosci.* 7, 395–408.
- Wakeham, S., Lee, C., 1993. Production, transport, and alteration of particulate organic matter in the marine water column. In: Engel, M., Macko, S. (Eds.), *Organic Geochemistry*. Springer US. https://doi.org/10.1007/978-1-4615-2890-6_6, 145–169.
- Wenke, A., Ferreira, G.B., Bullimore, S.A., Clark, S.A., Dörner, M., Embry, P., et al., 2021. Unlocking the cretaceous petroleum systems of the Norwegian sea. In: 82nd EAGE Annual Conference & Exhibition. European Association of Geoscientists & Engineers, pp. 1–5. <https://doi.org/10.3997/2214-4609.202010949>, 2021.
- Wesenlund, F., Grundvåg, S.-A., Engelschön, V.S., Thießen, O., Pedersen, J.H., 2022. Multi-elemental chemostratigraphy of Triassic mudstones in eastern Svalbard: implications for source rock formation in front of the World's largest delta plain. *The Depositional Record* 1–36. <https://doi.org/10.1002/dep2.182>, 00.
- Zastrozhnov, D., Gernigon, L., Gogin, I., Abdelmalak, M.M., Planke, S., Faleide, J.I., Eide, S., Myklebust, R., 2018. Cretaceous-paleocene evolution and crustal structure of the northern Vøring margin (offshore mid-Norway): results from integrated geological and geophysical study. *Tectonics* 37 (2), 497–528.
- Zastrozhnov, D., Gernigon, L., Gogin, I., Planke, S., Abdelmalak, M.M., Polteau, S., Faleide, J.I., Manton, B., Myklebust, R., 2020. Regional structure and polyphased Cretaceous-Paleocene rift and basin development of the mid-Norwegian volcanic passive margin. *Mar. Petrol. Geol.* 115.
- Zheng, X.-Y., Jenkyns, H.C., Gale, A.S., Ward, D.J., Henderson, G.M., 2013. Changing ocean circulation and hydrothermal inputs during Ocean Anoxic Event 2 (Cenomanian–Turonian): evidence from Nd-isotopes in the European shelf sea. *Earth Planet Sci. Lett.* 375, 338–348.